Cryogenic Normal Conducting RF Accelerators - Experiments That Enable High Brightness RF Guns

Valery Dolgashev

SLAC National Accelerator Laboratory

Seminar at the John Adams Institute for Accelerator Science at the University of Oxford, UK, 19 June 2017

U.S. DEPARTMENT OF ENERGY
Office of Science

NATIONAL ACCELERATOR LABORATORY

SLAC: Two Mile Linac

1962: Start of accelerator construction

1967: 20-GeV electron beam achieved

1989: The first linear collider, SLC operations begin, 50 GeV with electron and positron beams

2009: First light in the first Hard-X-Ray Free Electron Laser LCLS

Ongoing: Construction LCLS-II, Free-Electron-Laser based on CW superconducting linac

- Power-pulse compression using SLAC Energy Doubler (SLED), accelerating gradient increased to ~20 MV/m

11.4 GHz, Standing Wave-Structure

1C-SW-A5.65-T4.6-Cu-Frascati-#2

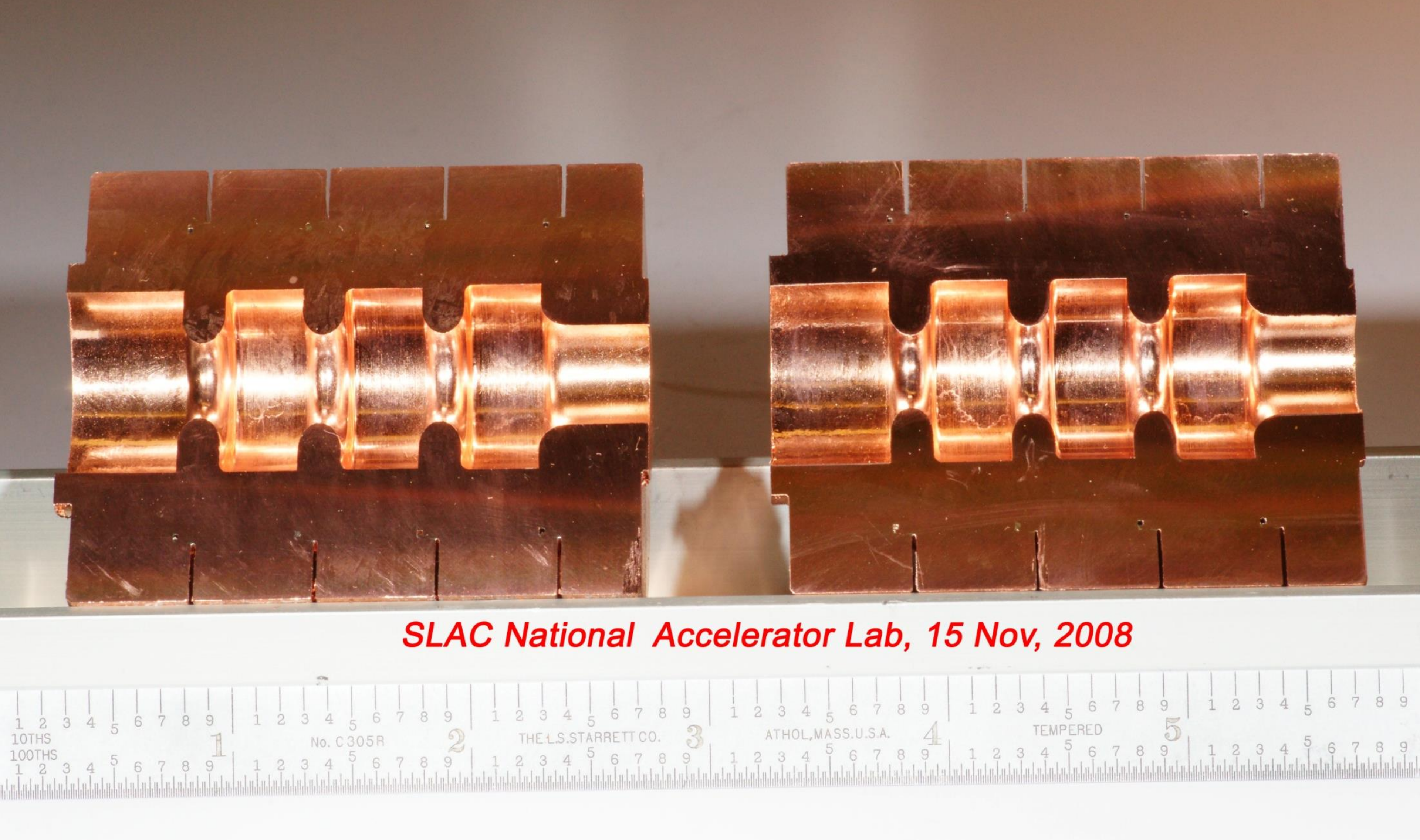

SLAC-KEK-INFN

Cell of Traveling Wave Accelerating Structure with damping waveguides, 11.4 GHz , CLIC prototype TD24

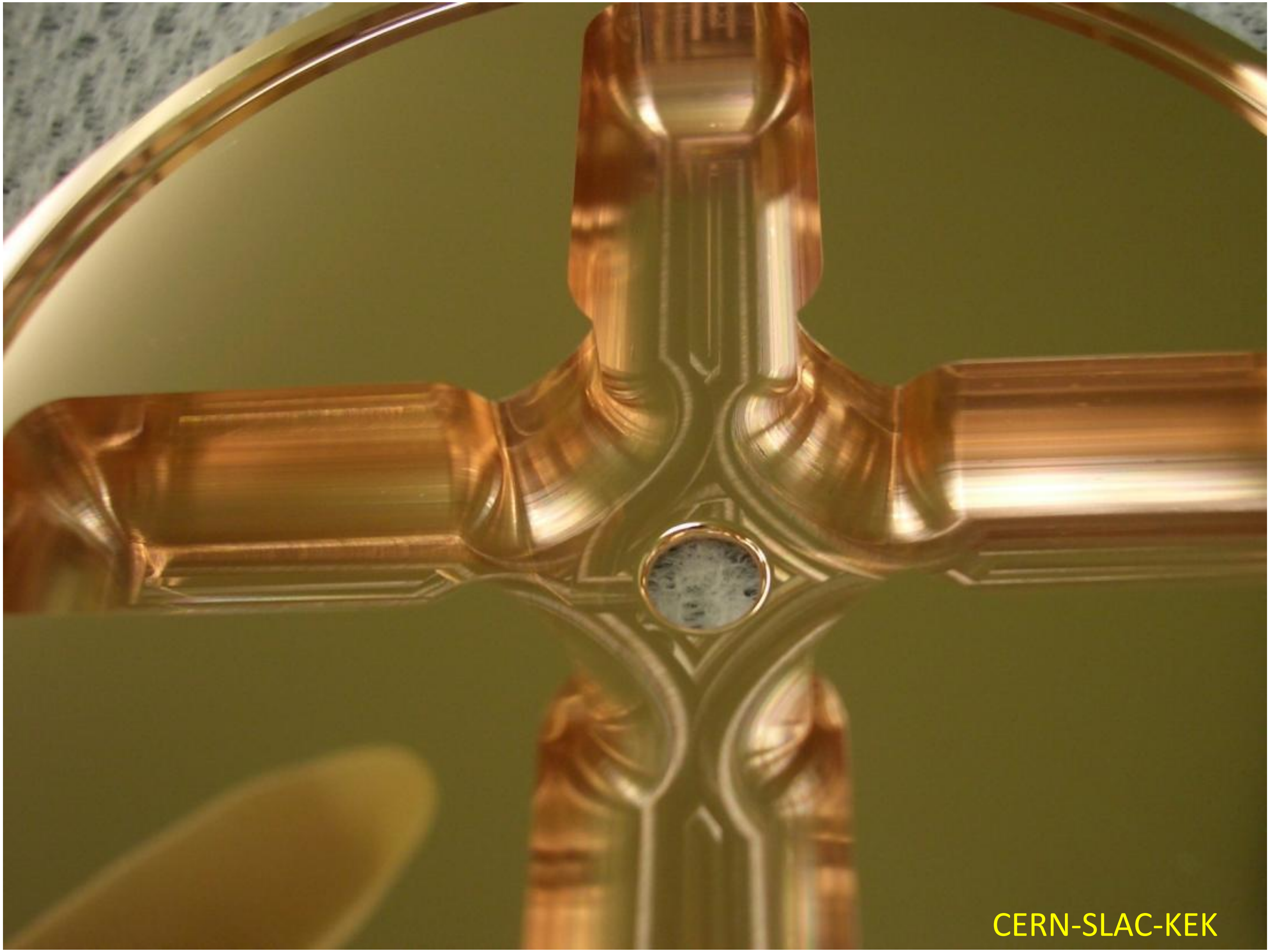

Traveling Wave Accelerating Structure with damping waveguides, 11.4 GHz , CLIC prototype TD18

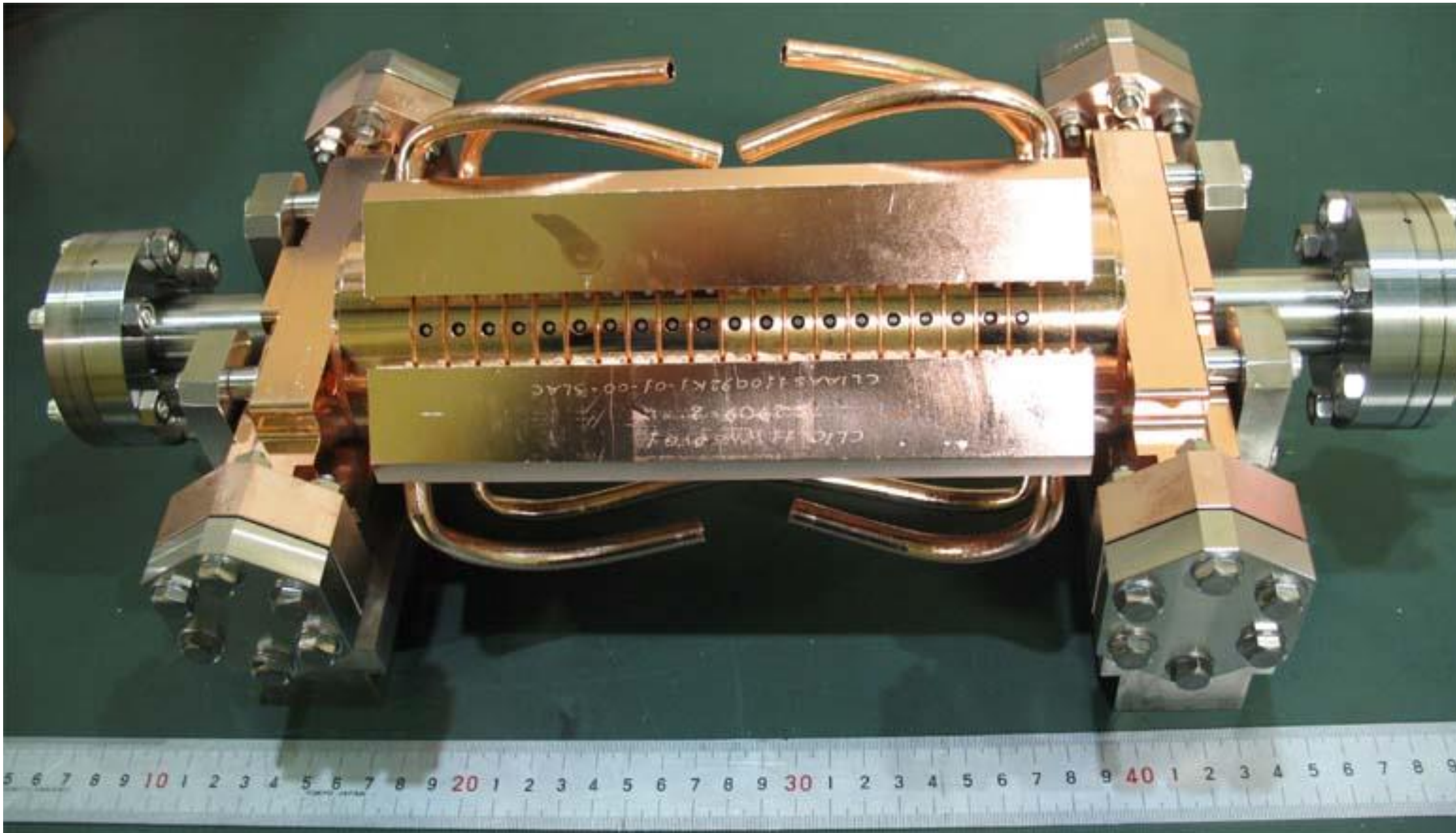

CERN-SLAC-KEK

11.4 GHz Standing Wave Structure with Photonic-Band Gap cell

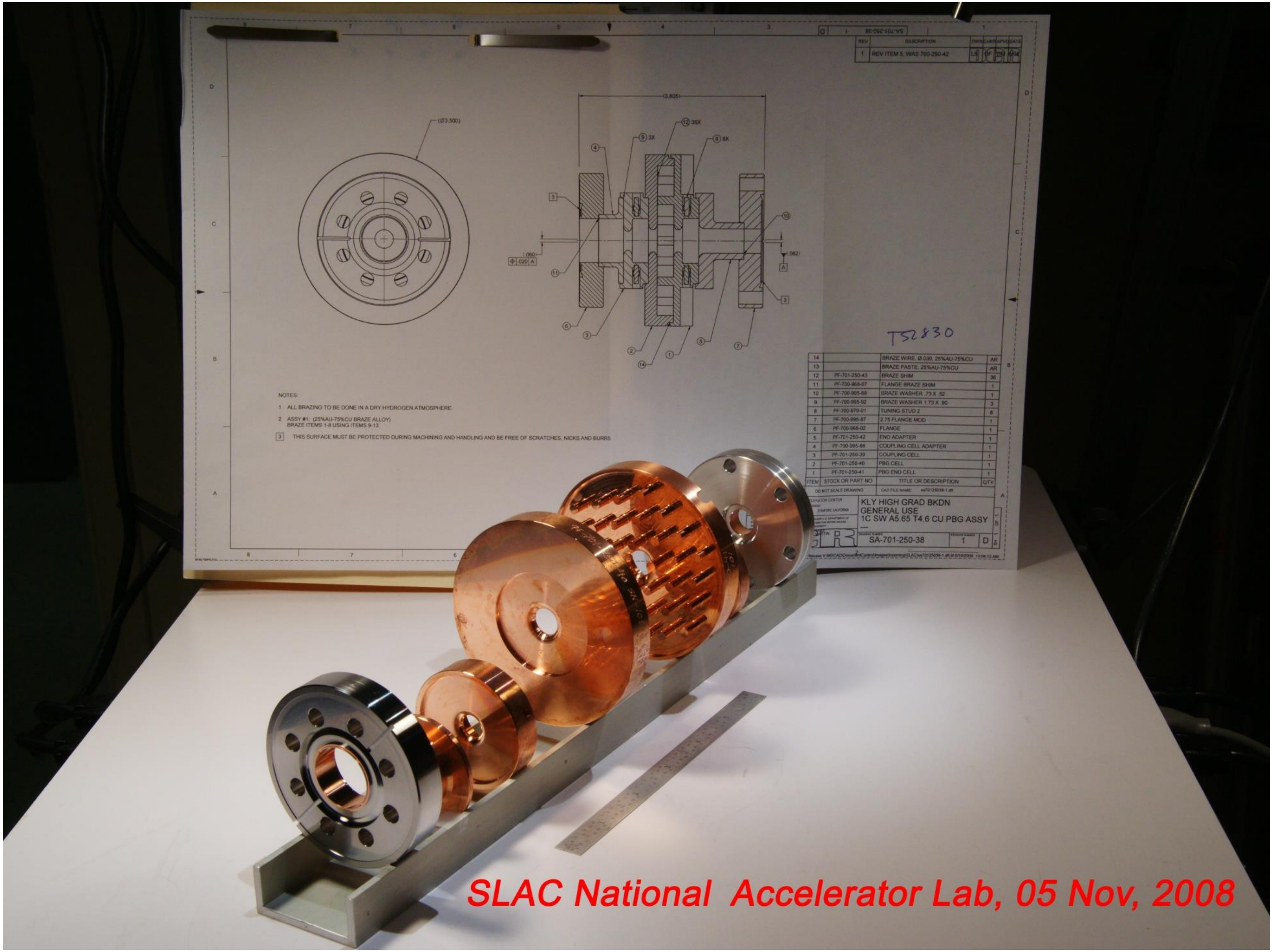

SLAC-MIT

Typical breakdown and pulse heating damage in standing-wave structure cell

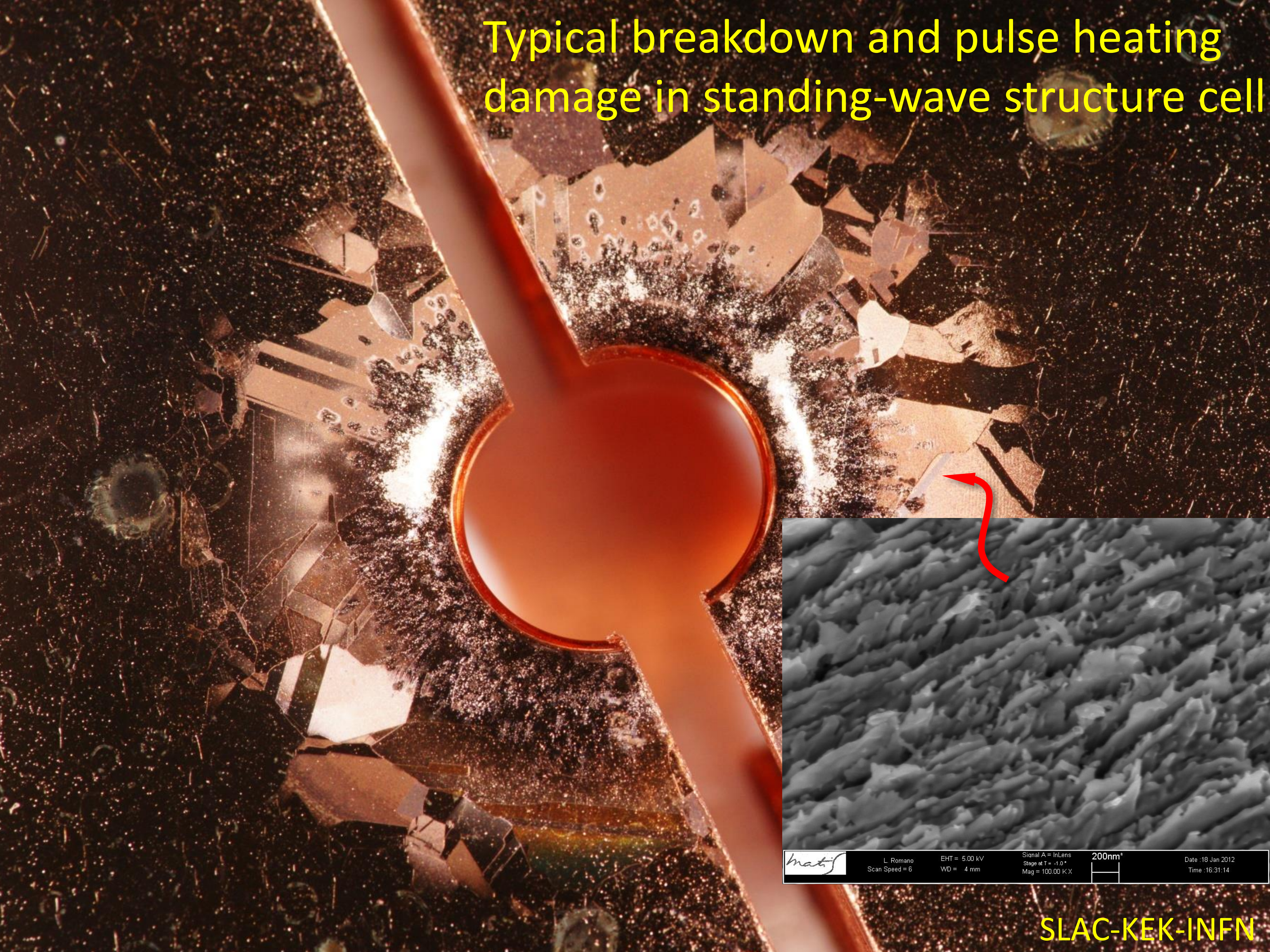

Outline

- Basic physics of ultra-high vacuum RF breakdown
- High-power test of copper cryogenic accelerating cavity
  - Understanding of dynamic Qo
  - Breakdown rates at 45K
- Application: cryogenic RF gun for FELs

SLAC Team: A. Cahill (UCLA), G. Bowden, J. Eichner, M. Franzi, A. Haase, J. Lewandowski, S. Weathersby, P. Welander, C. Yoneda, S. Tantawi

Study of Basic Physics of RF Breakdowns: Single Cell SW and Short TW Accelerating Structures

Goals

- Study rf breakdown in *practical* accelerating structures: dependence on circuit parameters, materials, cell shapes and surface processing techniques

Difficulties

- Full scale structures are long, complex, and expensive

Solution

- *Single cell standing wave (SW)* structures with properties close to that of full scale structures
- *Short traveling wave (TW) structures*
- Reusable couplers

We want to predict breakdown behavior for practical structures

Reusable coupler: TM_{01} Mode Launcher

Pearson's RF flange

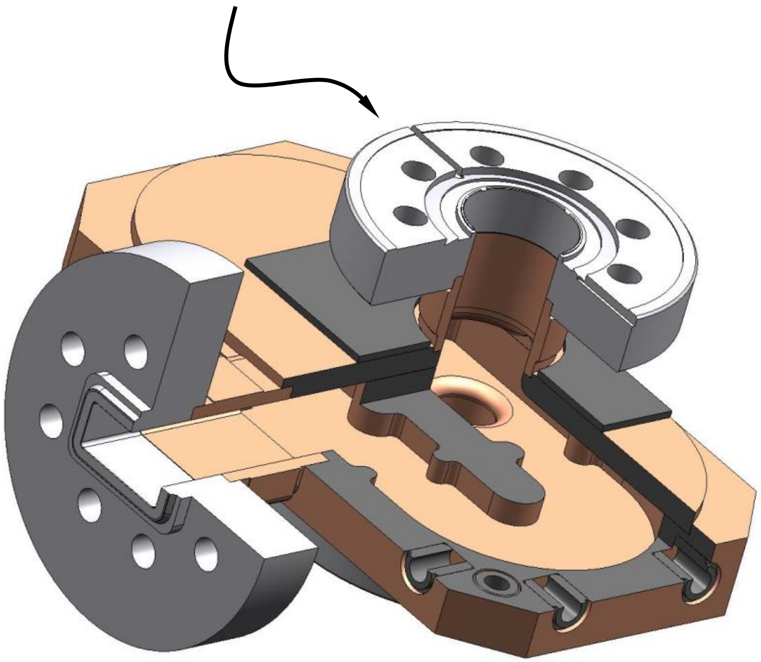

Cutaway view of the mode launcher

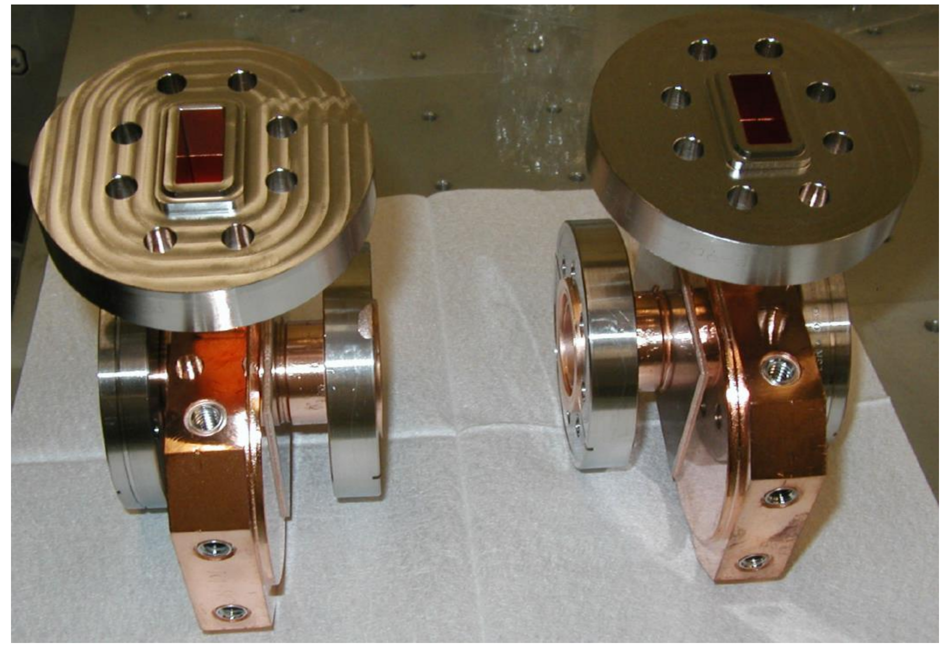

Two mode launchers

Surface electric fields in the mode launcher
E_{max}= 49 MV/m for 100 MW

S. Tantawi, C. Nantista

Current “state of the art”

- We practically can predict performance of heat-treated soft copper structures from drawings.
  - We found peak pulse heating to be good predictor of breakdown rate in simple, disk-loaded-waveguide type geometries.
  - We found “modified Poynting vector” to be a practical predictor of breakdown rate in more complex geometries.
- Motivated by correlation of peak pulse heating and breakdown rate we study hard cooper alloys and methods of building structures out of them.
  - We found hard Cu and hard CuAg have better performance then soft heat-treated copper.
  - As for now, hard CuAg had record performance for room temperature structures.
- We study clad metal and multi-layered structures and their construction methods. Idea is to study materials with designed properties.
- We started looking at process of initial conditioning:
  - In 3 CuAg experiments (1 soft and 2 hard) we observed unusual conditioning: breakdown performance on initial stages of conditioning was better than at final stage. Note that at this final stage the performance is better then in common soft-copper structures.
- We study new methods of breakdown diagnostics and autopsy, specifically on ion-beam-milling and X-ray microscopy.
- We started looking at breakdown physics at 100 GHz frequencies and above
- We study breakdown in cryo normal conducting structures

Normal Conducting Cryogenic Structure

We conjecture that the breakdown rate is linked to movements of crystal defects induced by periodic stress. Pulse heating creating some or, possibly major part of this stress. So, by decreasing crystal mobility and increasing yield stress we will reduce the breakdown rate for the same gradient. We want to do this by cooling a cavity to to 4…100 K.

- Pros:
  - Resistivity decreased thus reducing rf power required to sustain the gradient.
  - Thermal conductivity increases and thermal expansion decreases thus decreasing stress due to pulse surface heating
  - Mobility of the crystals decreased, yield stress increases.
  - Vacuum pumping between breakdowns is improved.
- Cons:
  - Since the cavity acts as a cryogenic vacuum pump any vacuum leak or other source of gasses could contaminate high field surfaces.
  - Due to reduced cooling efficiency at low temperature, overall efficiency of the system decreased and makes high repetition-rate operation problematic.

Precision Measurements of Metal Properties at Low Temperatures: Sami’s TE0 Dome Cavity

- Flat copper samples of varying purity and grain size.
- Goes down to ~3K.

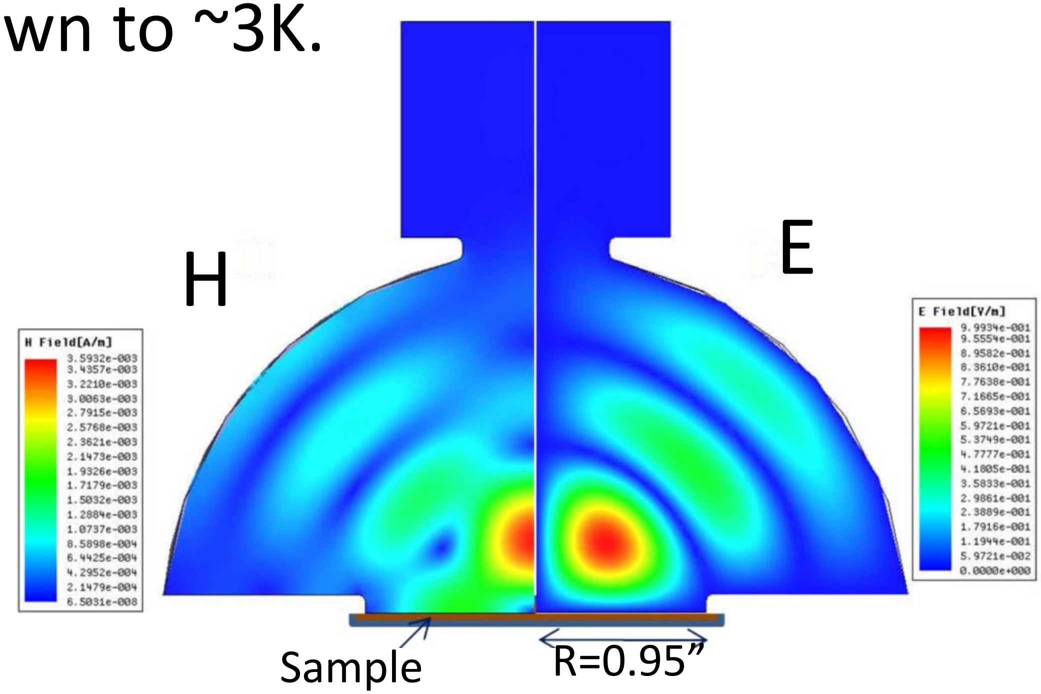

Sami Tantawi, Jiquan Guo

Results for X-Band TE Dome Cavity Cu samples

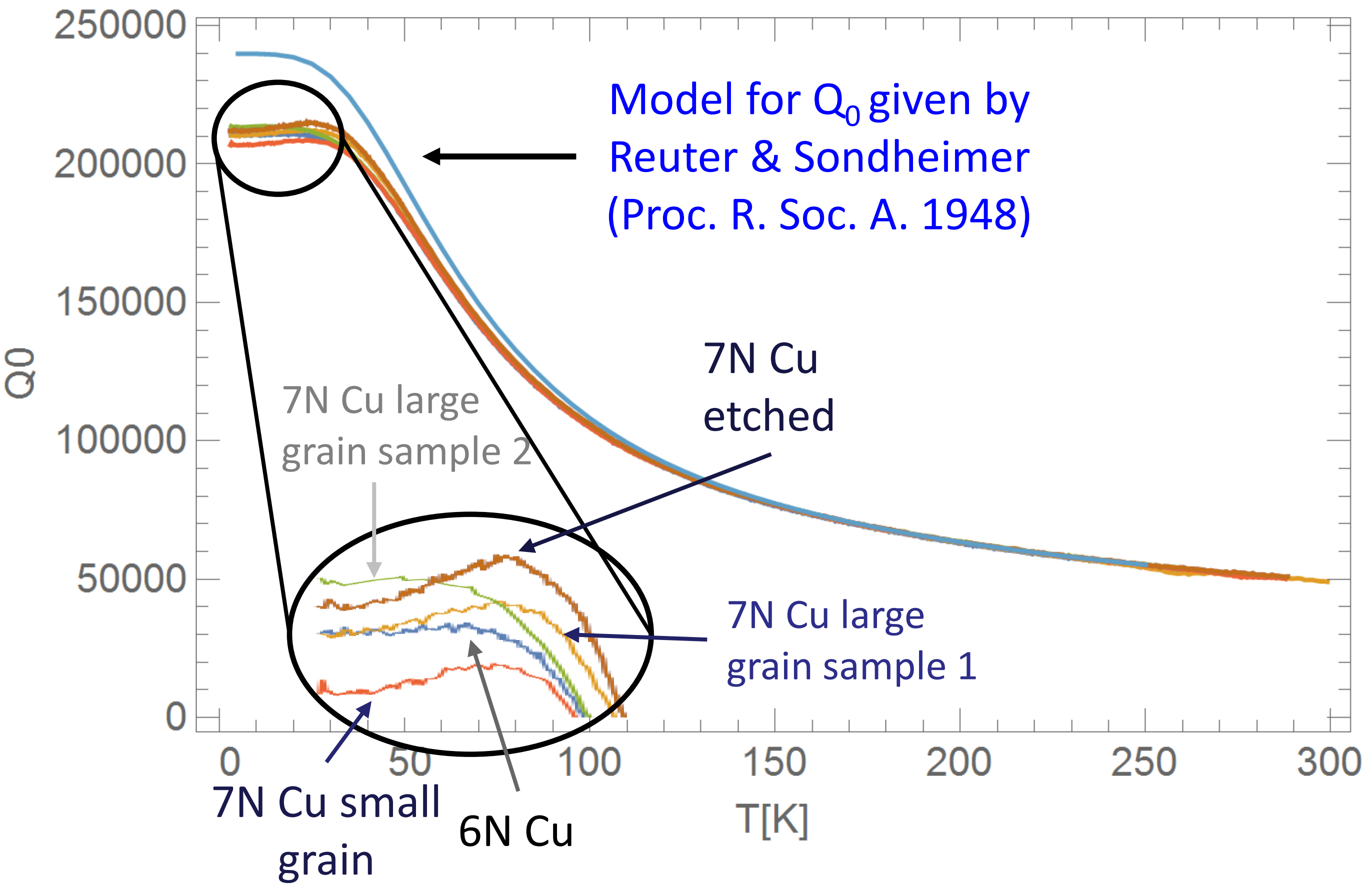

- The copper samples were 6N and 7N purity with large and small grain sizes.
- One 7N sample was etched
- Notice that there is very small difference over a large range of samples

Y. Higashi (KEK, OIST), Jiquan Guo, Sami Tantawi

1C-SW-T2.75-A2.0-Cryo-Cu, 11.3925 GHz
10 MW rf input (lossy 2nd order driven calculation)

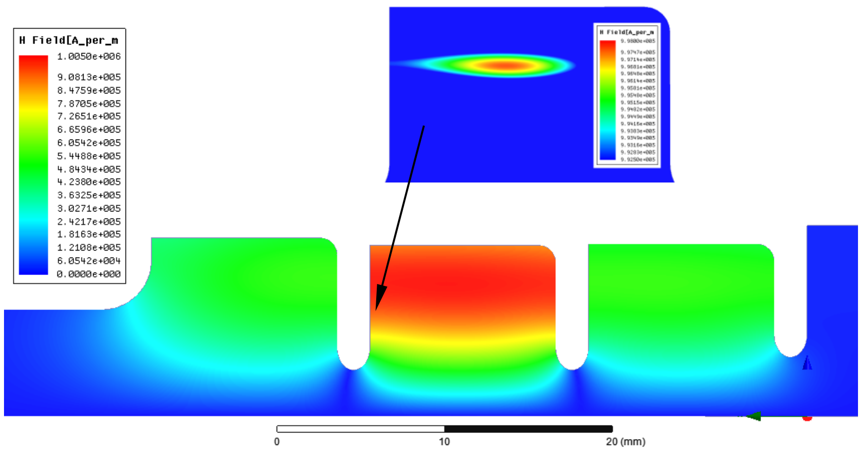

Maximum magnetic field 992.5 kA/m
(SLANS 993.2 kA/m)

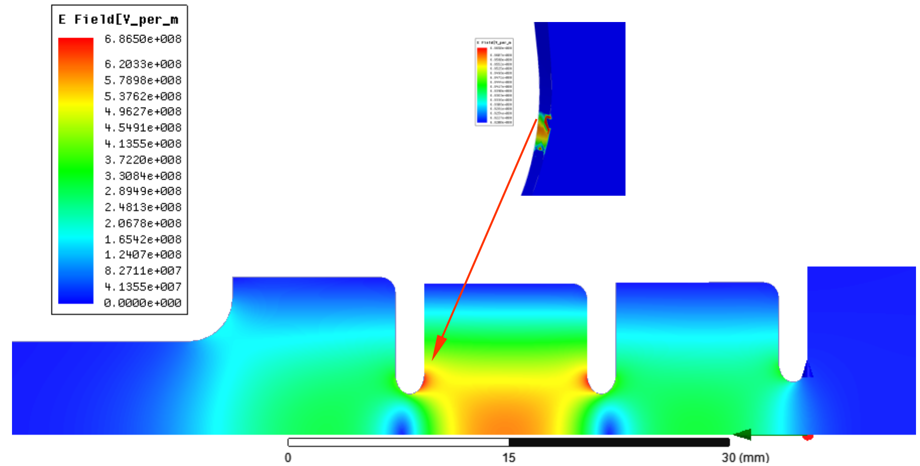

Maximum electric field 686 MV/m
(SLANS 678 MV/m)

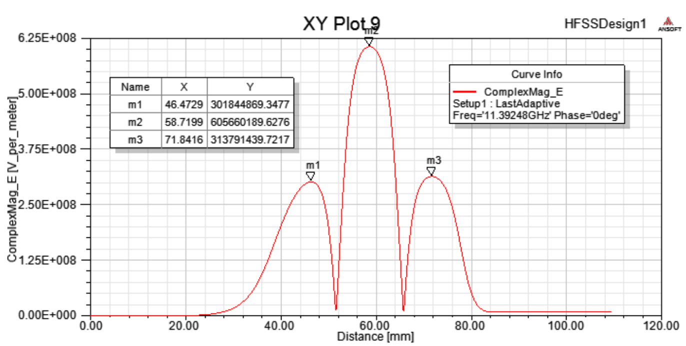

Coupler-cell on-axis field is ~4% high vs. end-cell field,
Peak field on axis 605.7 MV/m (SLANS 605.7 MV/m)

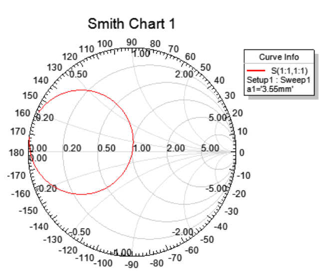

Slightly over coupled with
beta= 1.00488

$$Q := \frac{11.394}{0.00114}$$

$$Q = 9.995 \times 10^{3}$$

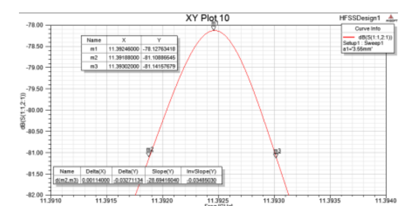

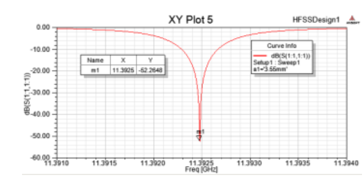

F=11.3925 GHz (SLANS 11.9340 GHz)

V.A. Dolgashev, SLAC, 14 March 2011

Design Q_o, coupling and gradient *vs.* temperature

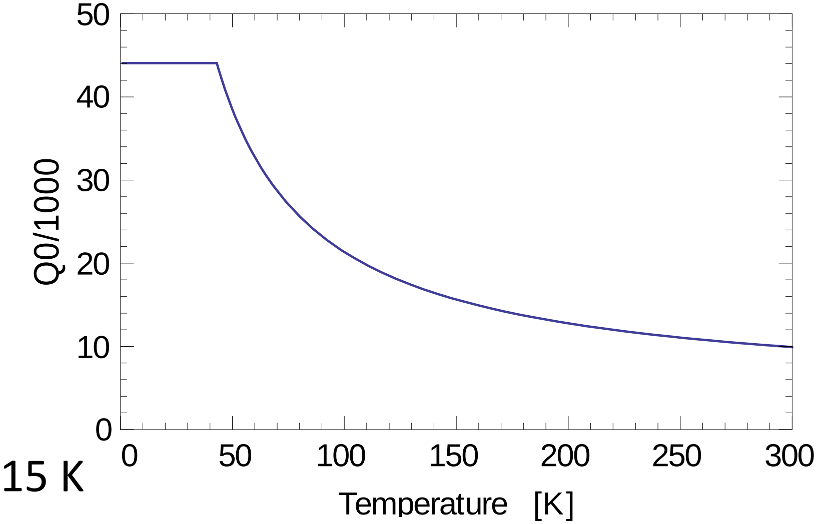

Designed to be critically coupled at 96.15 K

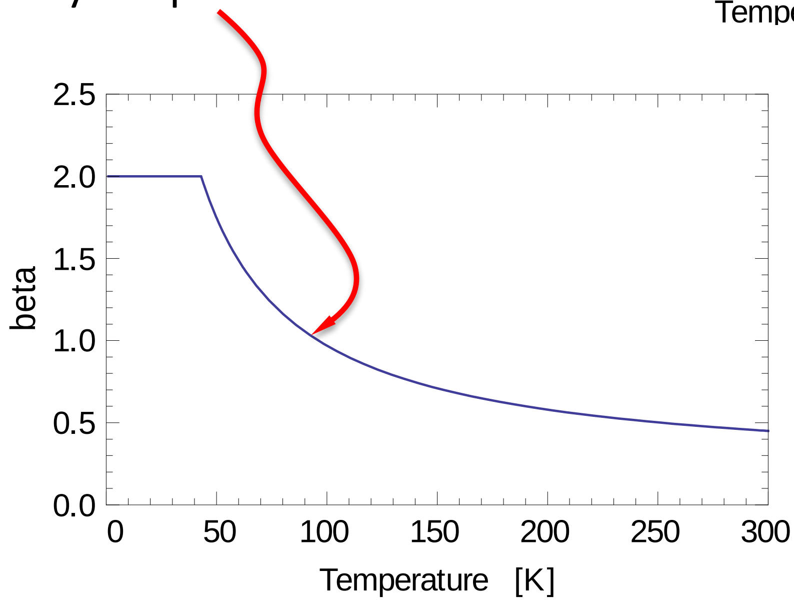

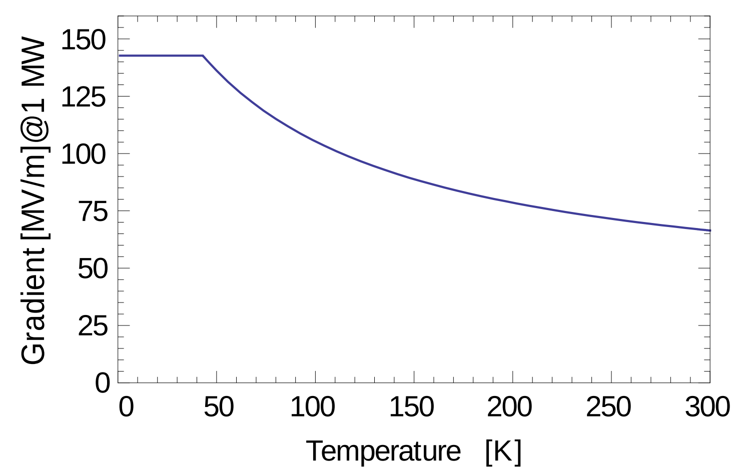

Cryo Structure Setup

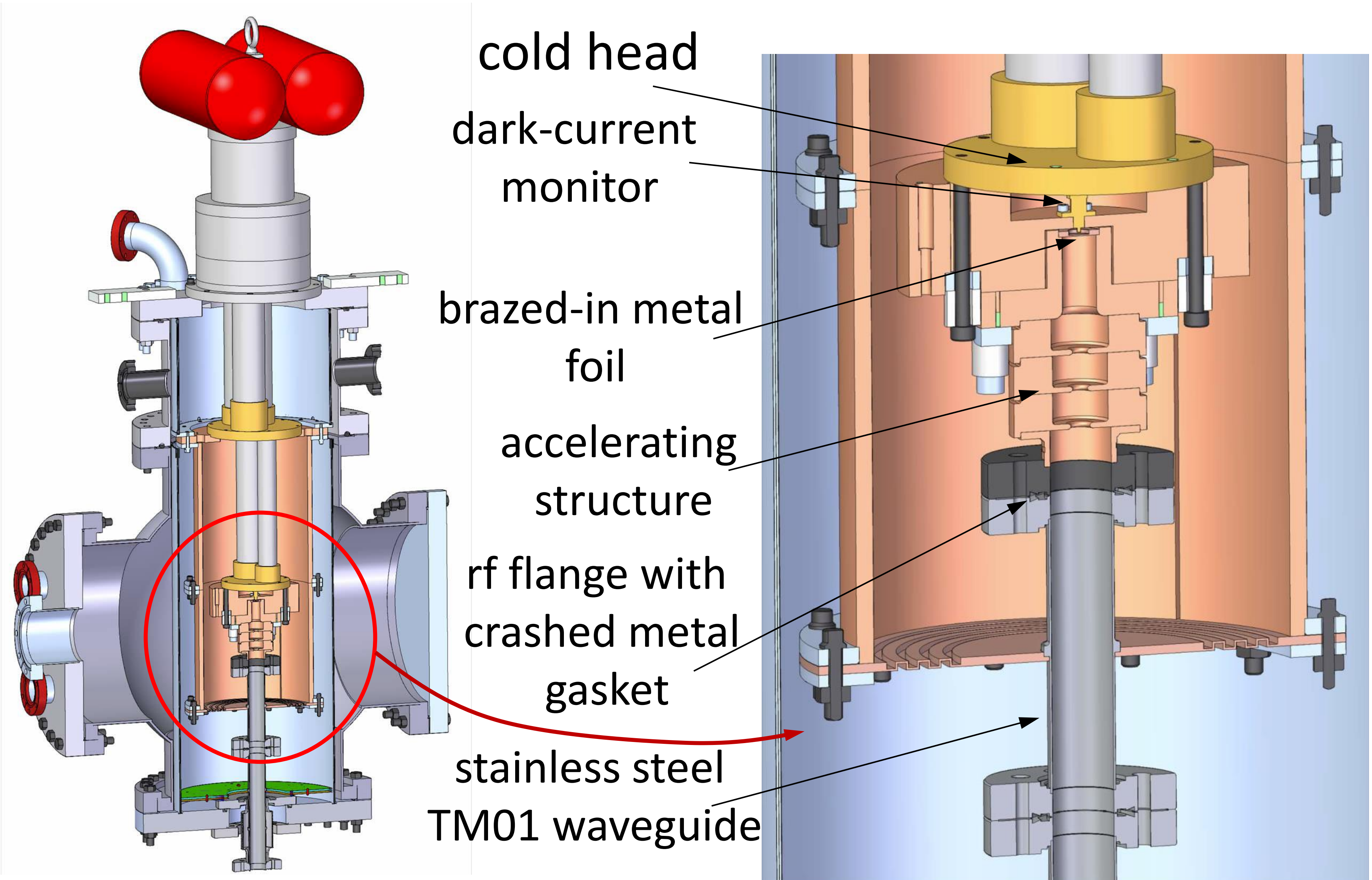

Cryostat assembly

Beadpull test of 1C-SW-T2.75-A2.0-Cryo-Cu-#2

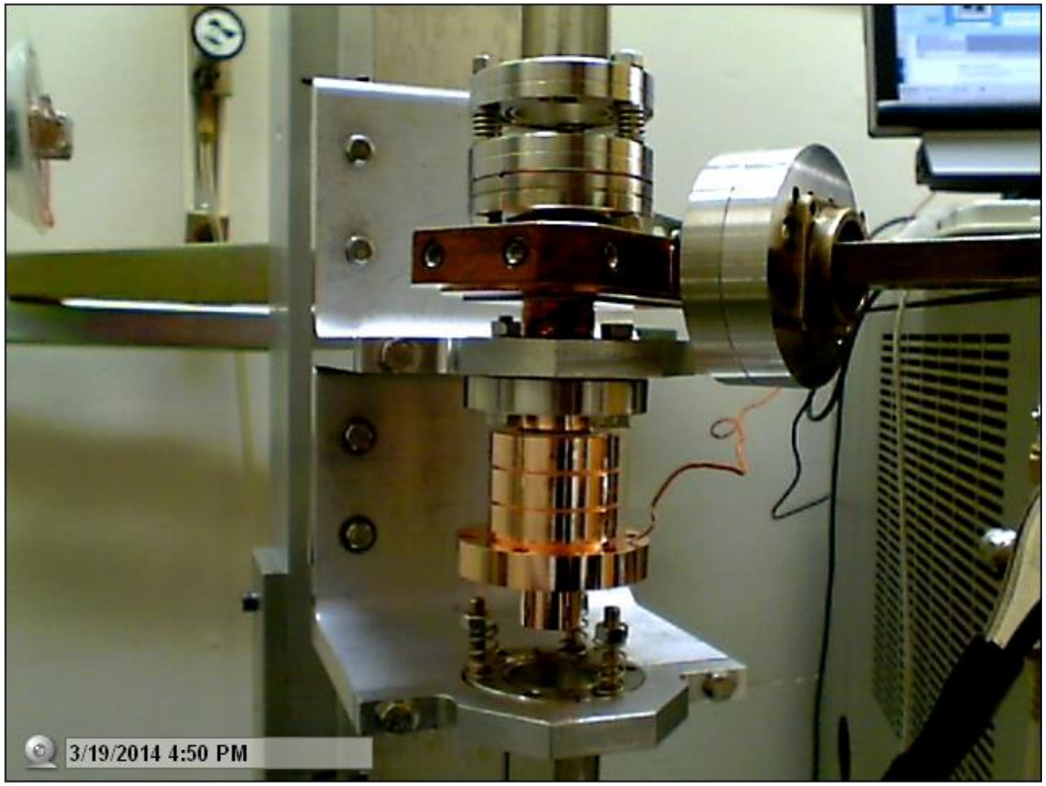

Beadpull setup

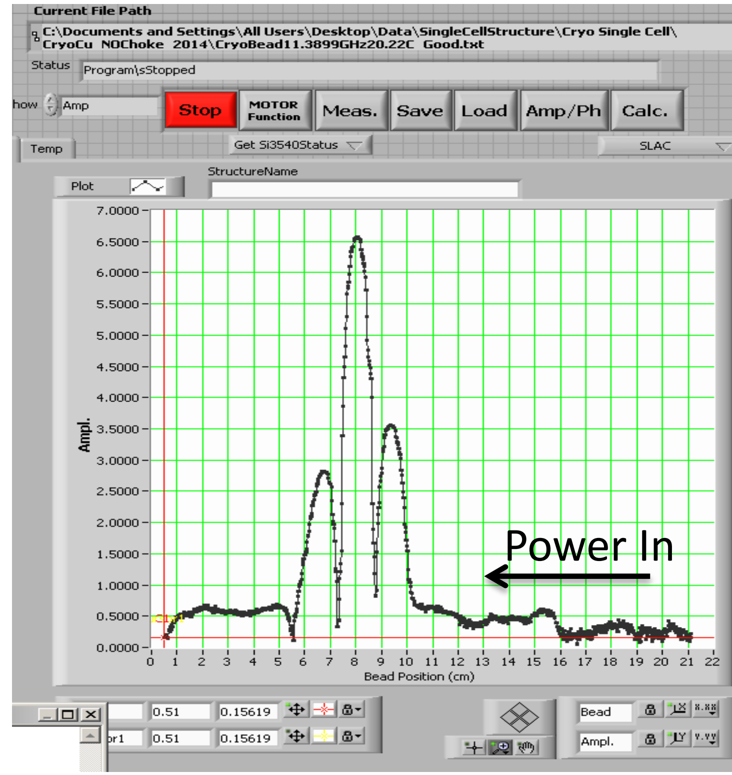

Measured on-axis field profile

Fitting measured signals by changing Qo

jj/njj=7/30 beta = 0.9 Qo=13680. Qext:15200 Ql=7200.

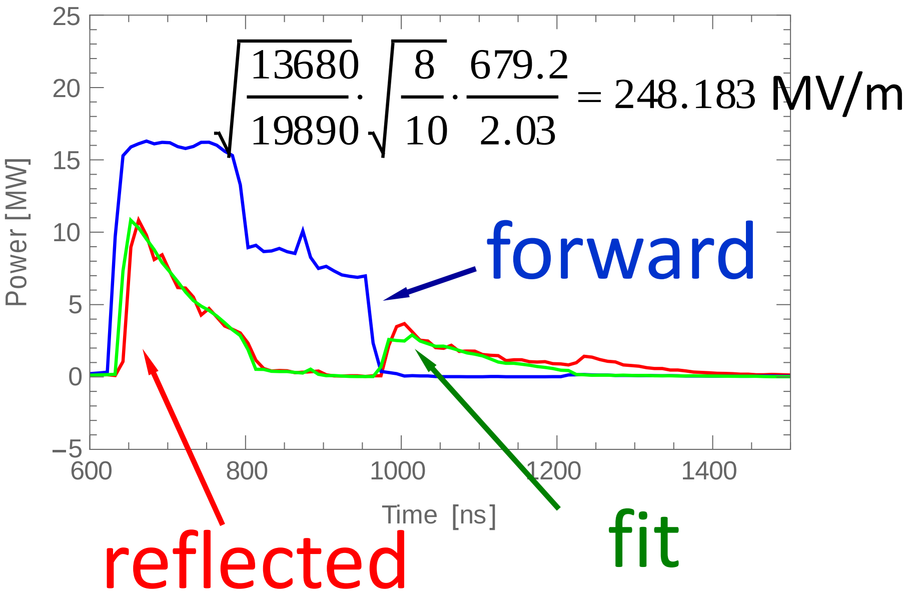

jj/njj=9/30 beta = 1.1 Qo=16720. Qext:15200 Ql=7961.9

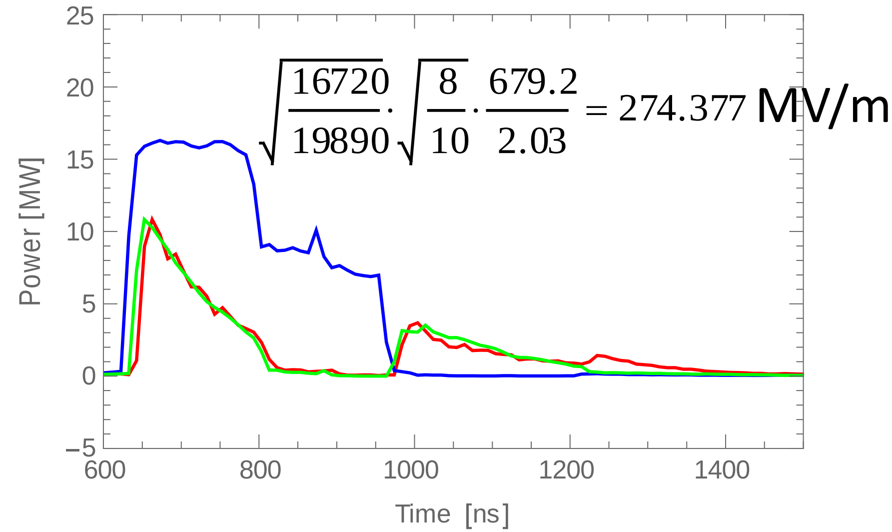

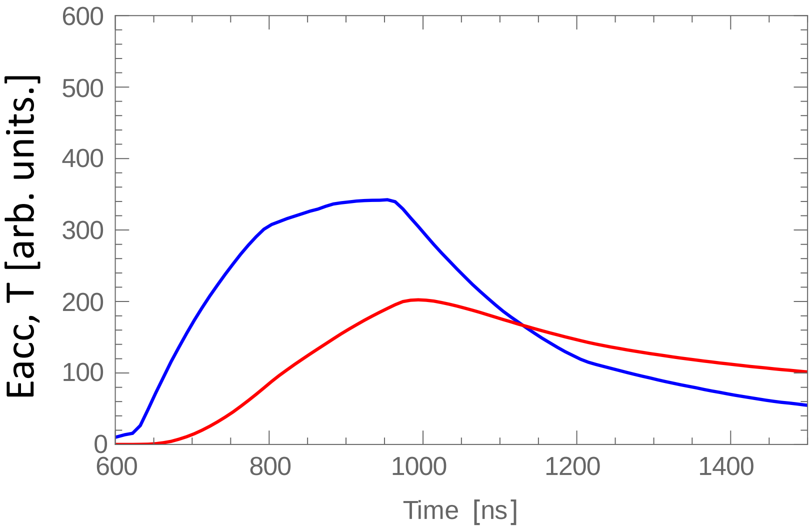

$Q_{loaded} = 7200$

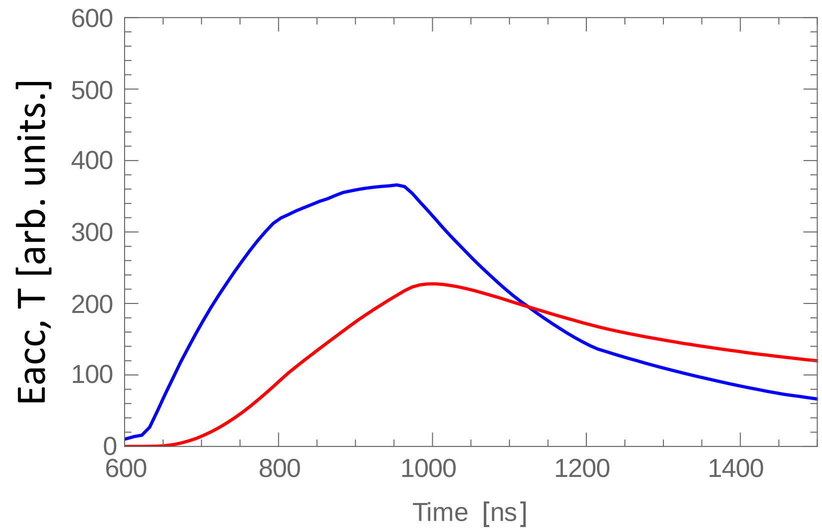

$Q_{loaded} = 7961$

Obtaining Q_{loaded} from decay of downmixed reflected signal

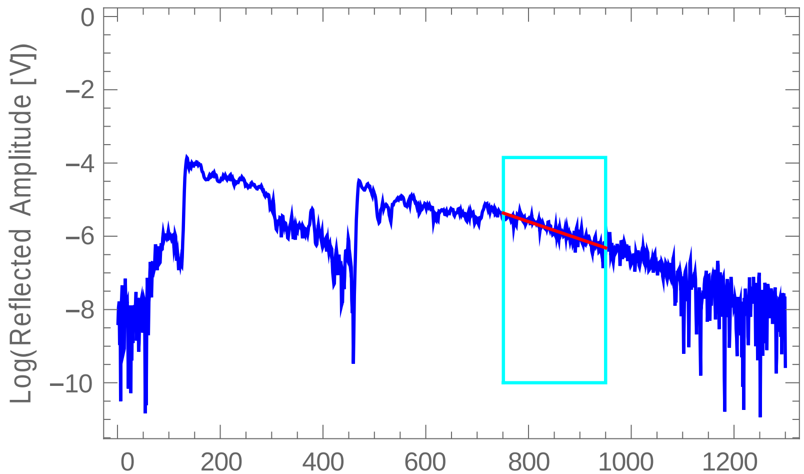

Amplitude of reflected signal

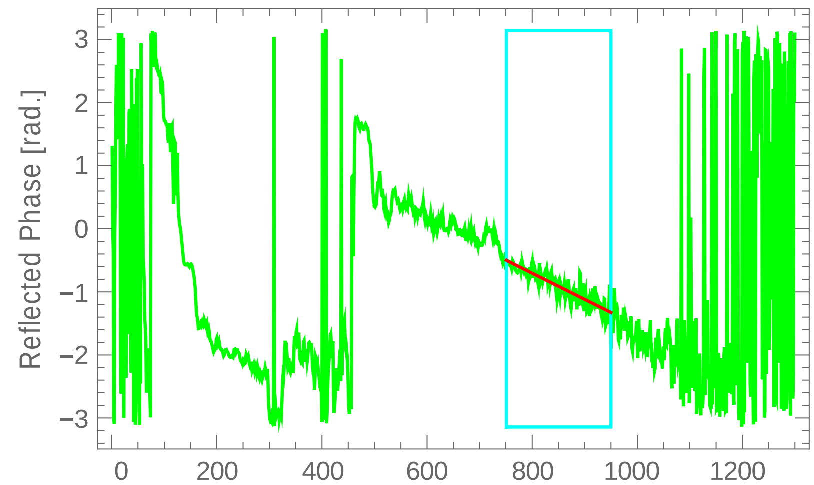

Phase of reflected signal, raw data

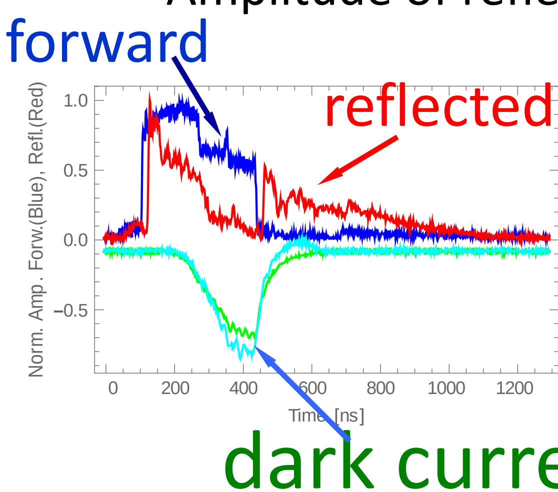

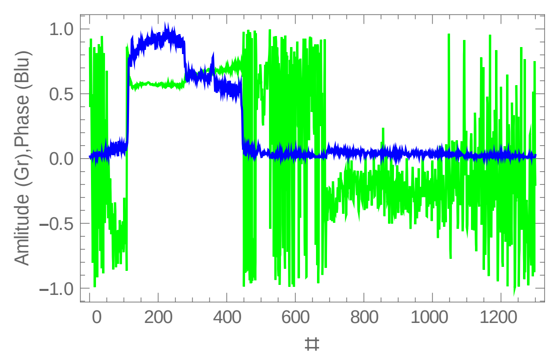

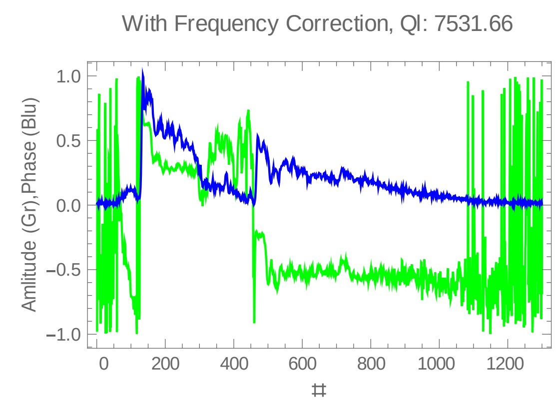

Q_{loaded} = 7531 is consistent with fit of peak-power meter signals

V.A. Dolgashev, SLAC, 18:22, 23 February 2015

Assuming design dependence of Qo vs. frequency, estimated temperature for Qo=15000 is 155 K while sensor shows 45 K

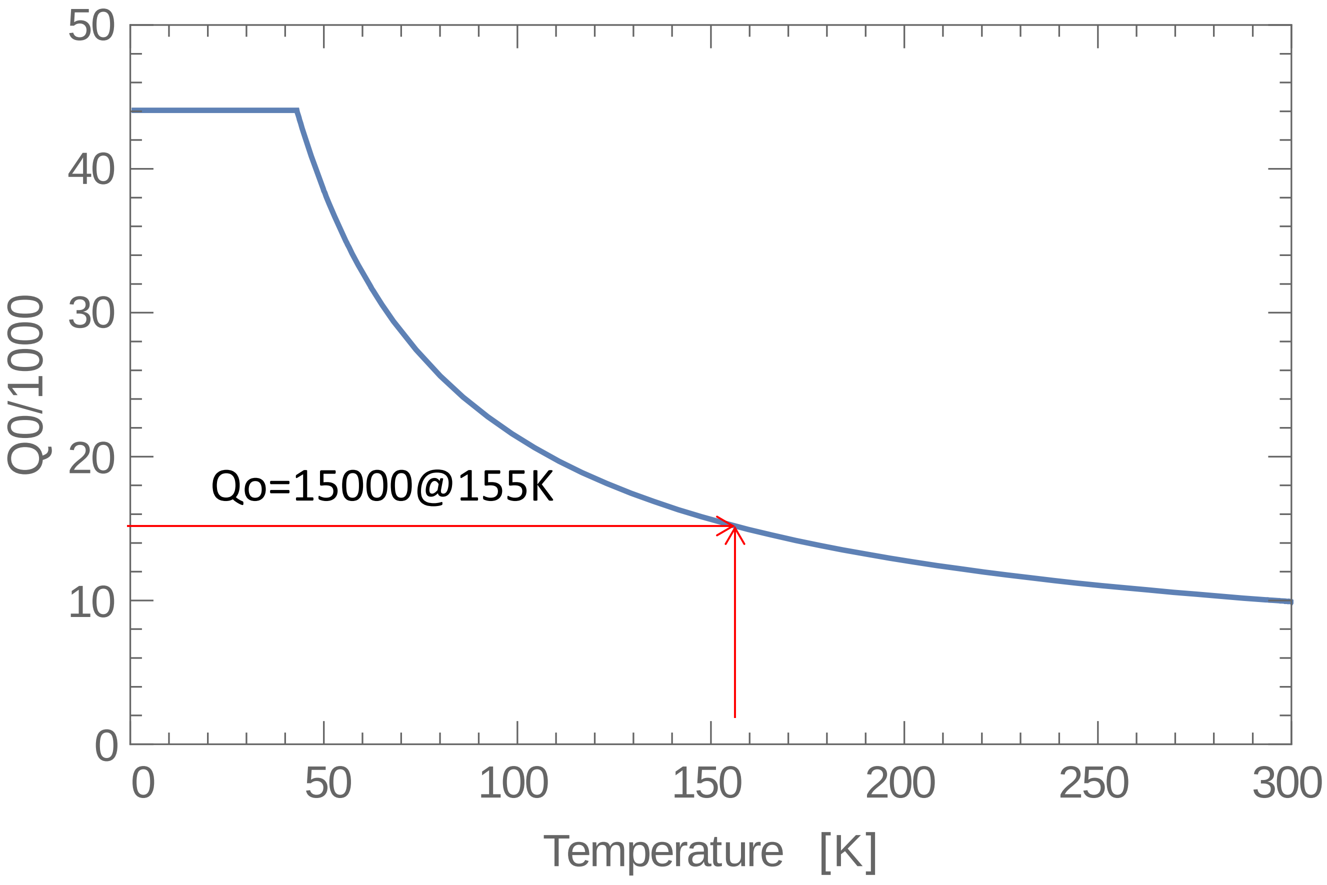

Performance of normal conducting cryo structure at 45 K assuming constant Qo obtained from fitting of the power signals, not from temperature sensor, *first breakdowns*

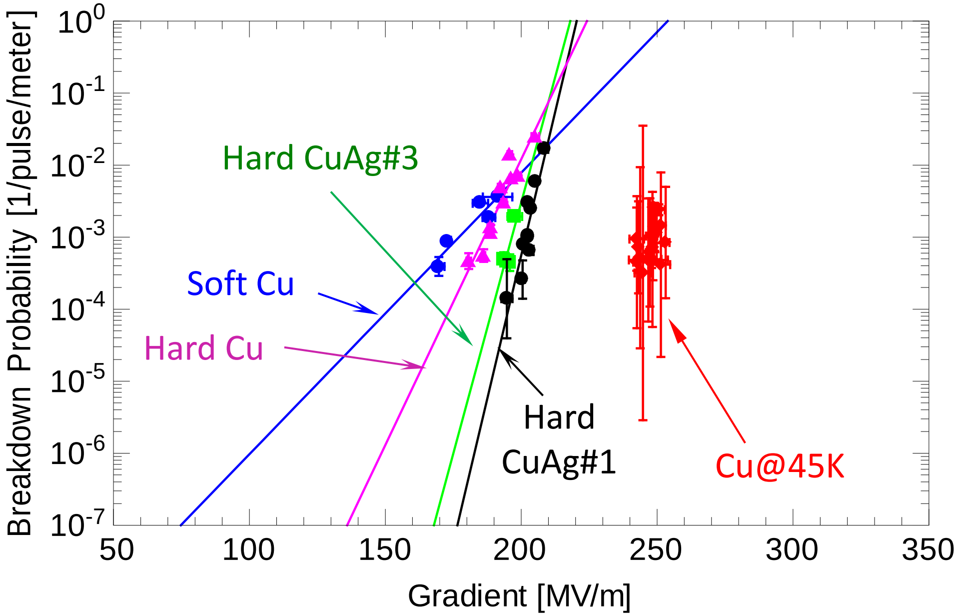

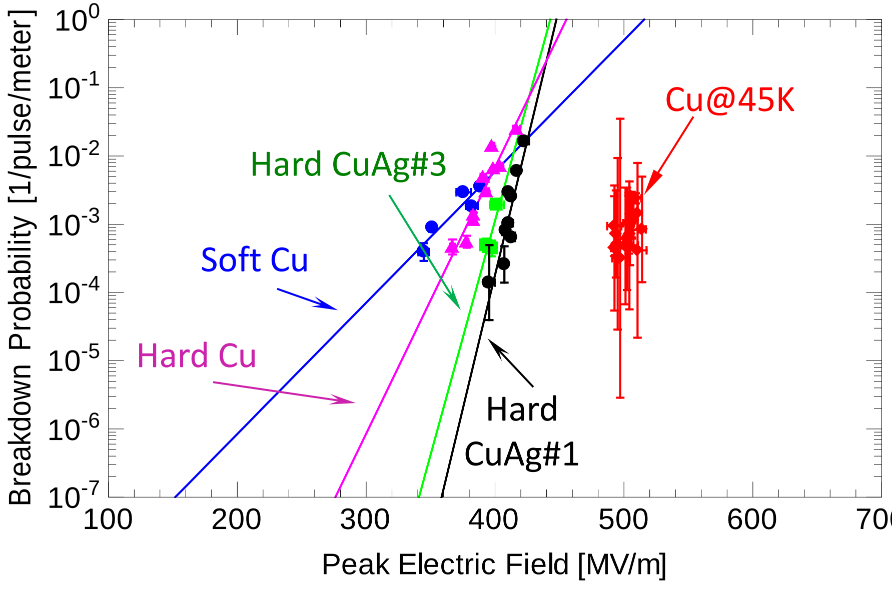

For the breakdown probability 10^{-3} .. 10^{-4} 1/pulse/m cryo structure clearly outperforms record data from hard CuAg obtained in initial stages of conditioning. CuAg on final stages of conditioning very similar to hard Cu.

To find accelerating gradient, we need to understand the discrepancy between Qo measured by network analyzer and extracted from high power signals

Method:

- Re-measure the cavity with a network-analyzer after processing
- Improve diagnostics and perform low- and high-power measurements using klystron rf pulse

Results of Low Power Measurements Performed After High Power Test, 1C-SW-A2.75-T2.0-cryo-cu-SLAC-#2: Qo of accelerating structure is lower then Qo of dome cavity, but the difference is not as dramatic as expected from high power data

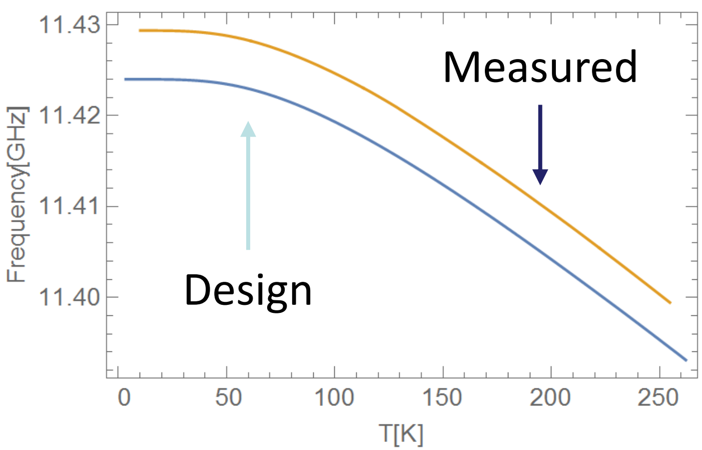

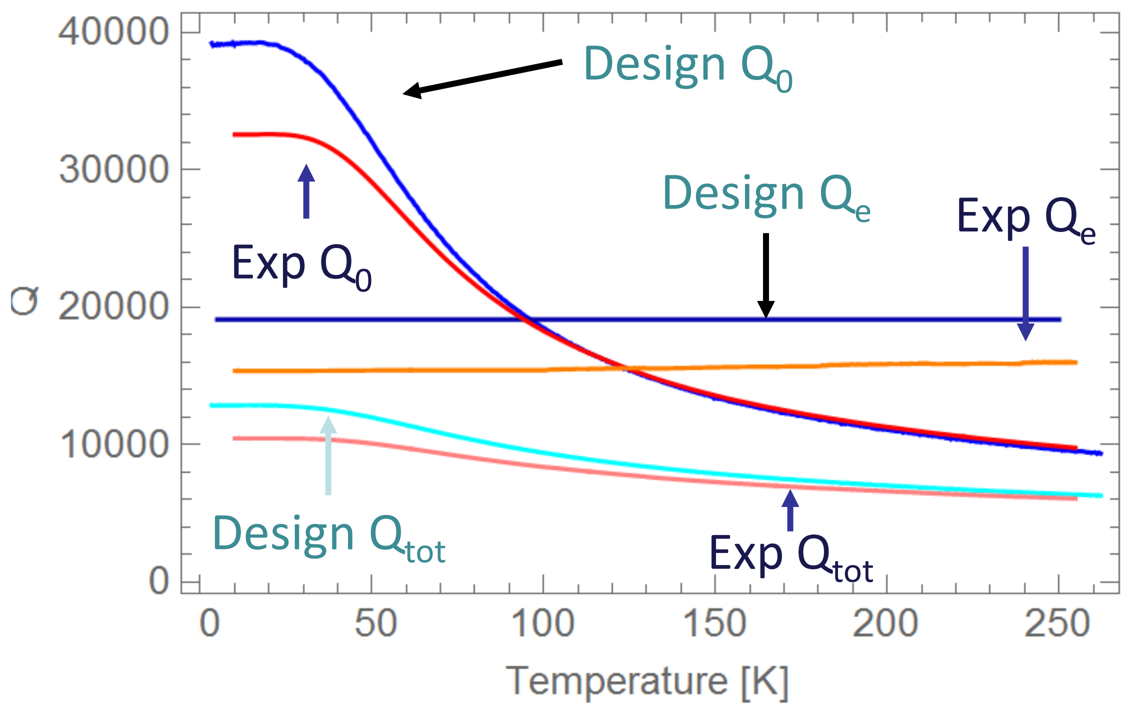

Design parameters versus measured

Matt Franzi, Jim Lewandowski

Q_0 is Different for Different Modes in Processed 1C-SW-A2.75-T2.0-Cryo-Cu-SLAC-#2

- We noticed that the increase in Q_0 with temperature varies between the three modes (0, π, π/2) of the Cryo Cavity.
- We hypothesize this is due to damage from high power experiments: the π mode has highest field in center cell and has lowest Q_0, π/2 has nearly no field in center cell and has the highest Q_0

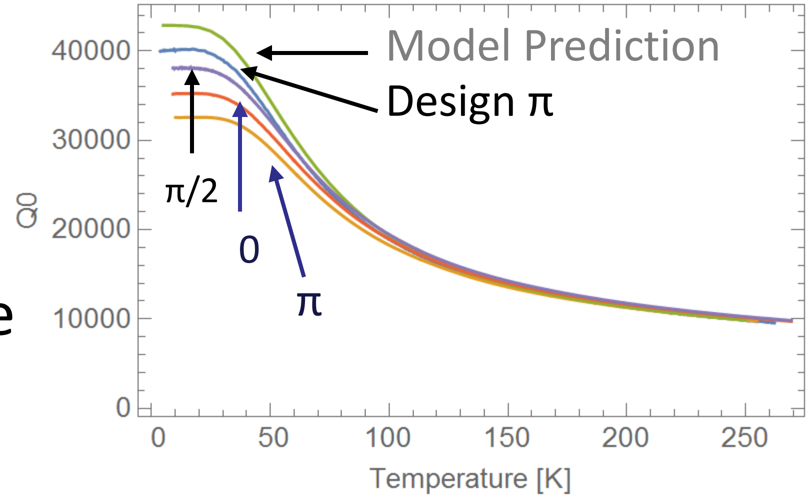

Q_0 values in cryo cavity compared to copper in TE dome cavity and analytic value for max Q_0 value

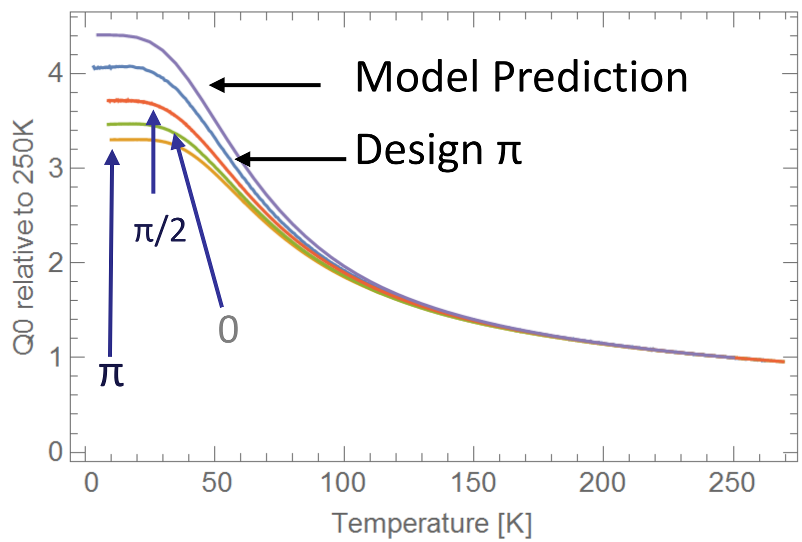

Data from above plot normalized to Q_0 value at 250K to illuminate trends

Matt Franzi,
Jim Lewandowski

Study of Dynamic Qo Using Klystron RF Pulse

- We improved accuracy and dynamic range of rf diagnostics.
- With this improved diagnostics, we systematically measured Qo at both low- and high- klystron power *vs.* temperature, repetition rate, pulse length, pulse shape, dark current.
- We build a circuit model of whole rf network, from klystron to cavity to understand its behavior.
- We build a circuit model of the cavity with Qo changing during the pulse. We fit the rf and dark current signals with this model using dramatic dependence of the dark current on surface fields as a field probe.
- We re-processed the rf breakdown data using this new model to find accelerating gradient.

Low power data matches constant Q_0 circuit model; high power data shows disagreement

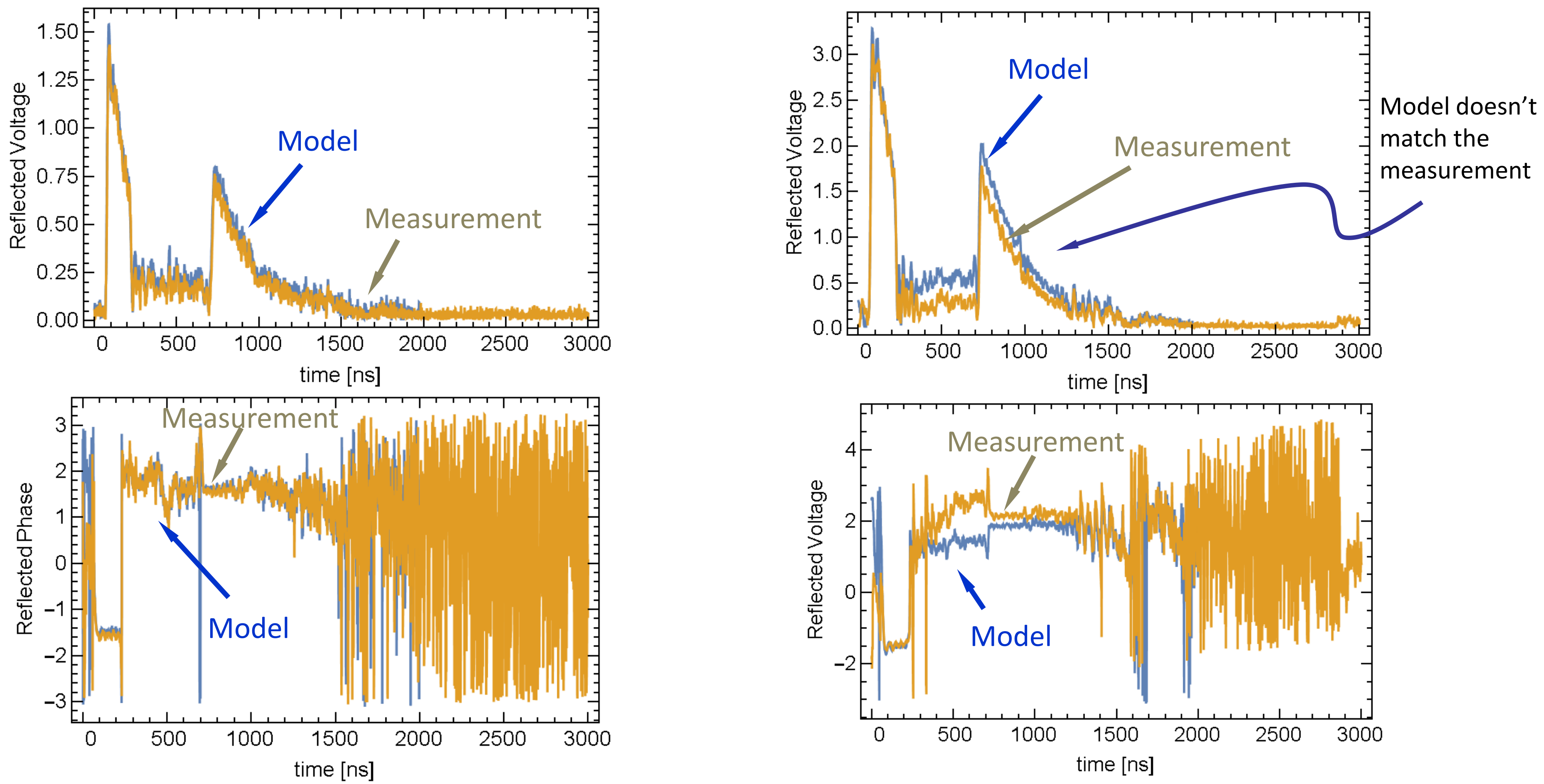

Low Power

High Power

At low power the rf signals measured and calculated with a linear circuit model match. At higher power they clearly different. The example is for cavity temperature of 25 K, 10 Hz repetition rate, and shaped pulse with 500 ns flat part.

A.Cahill *et al.*, "Quality Factor in High Power Tests of Cryogenic Copper Accelerating Cavities," NAPAC 16

Calculating Accelerating Gradient With Time-Dependent Q_0

- Q_0 and ω_0, the resonant frequency, are allowed to vary during the rf pulse.
- The differential equation describing the electric field:

$$\frac{d\tilde{E}}{dt}\left(\frac{\omega_0}{Q_E} + \omega\left(\frac{1}{Q_0} - 2i\right)\right) + \tilde{E}\left((\omega_0^2 - \omega^2) - i\omega\left(\frac{\omega}{Q_0} + \frac{\omega_0}{Q_E}\right)\right) = \sqrt{\frac{8P_{\mathrm{in}}\omega_0^3}{\mu_0 Q_E}}$$

- Magnitude and rate of the Q_0 decay is chosen to match the measured dark current and rf signals.

Processing History of 1C-SW-A2.75-T2.0-cryo-cu-SLAC-#2

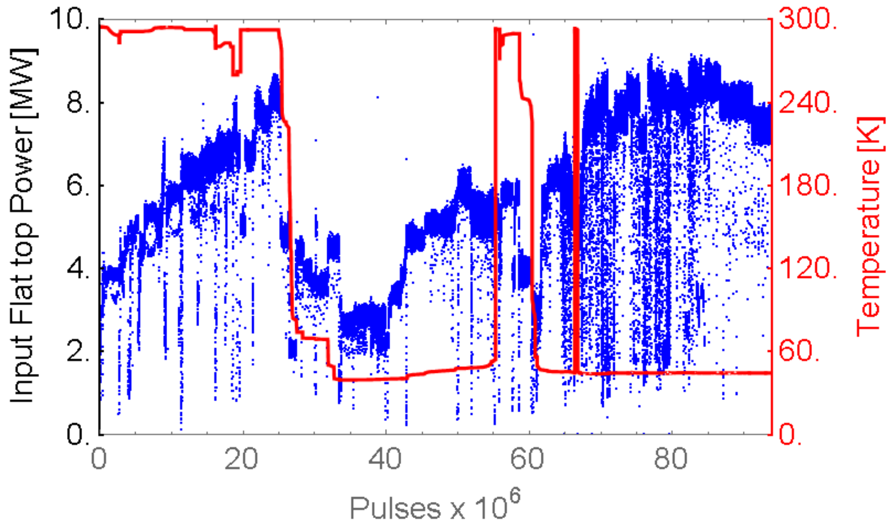

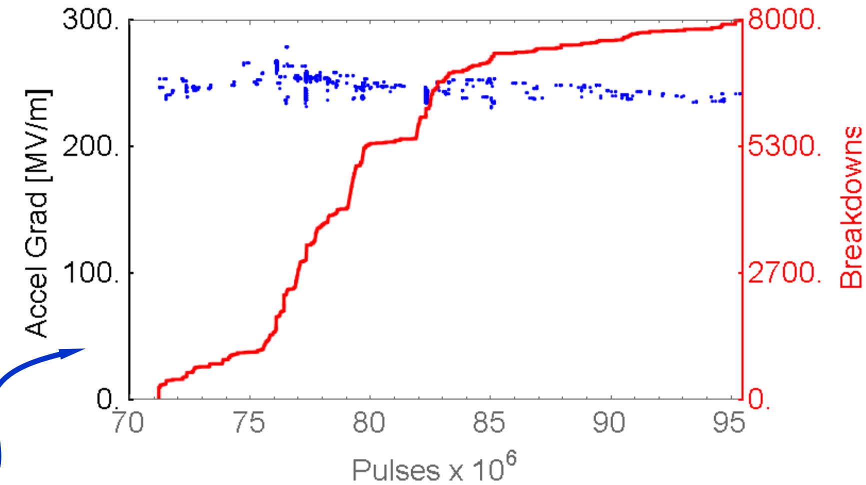

Zoom in of the data used to calculate rf breakdown statistics

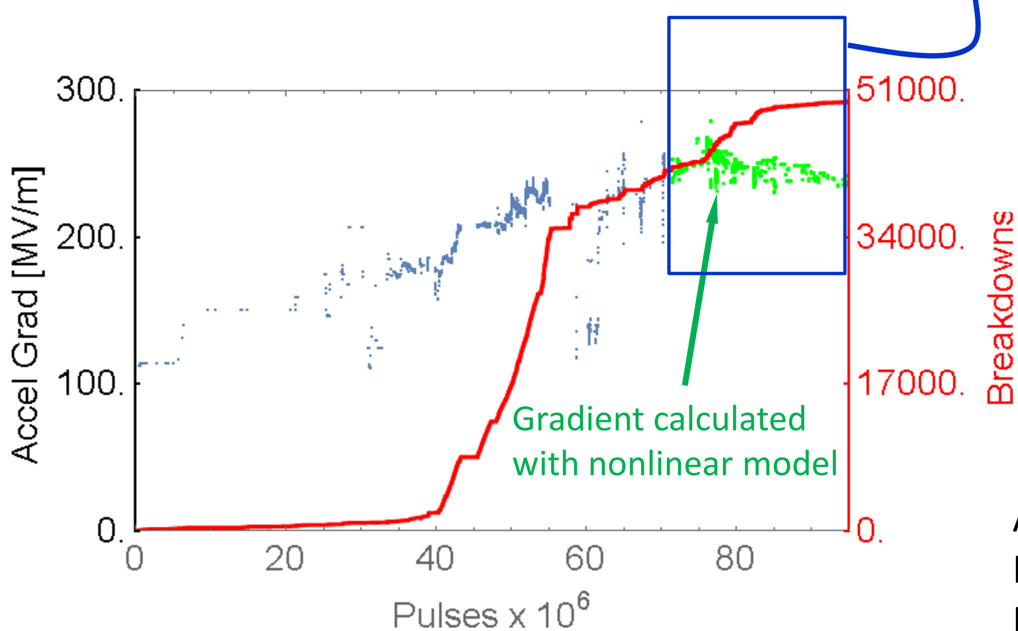

A. Cahill *et al.*, "Ultra High Gradient Breakdown Rates in X-Band Cryogenic Normal Conducting Rf Accelerating Cavities," IPAC 17

Example Pulse From Breakdown Rate Measurement

Shaped pulse with 150 ns flat part. Cavity temperature is 45 K.
Average power during flat part of the pulse: 7.6 MW.
Qo decreases from 30,400 to 19,700.
Accelerating Gradient: 247 MV/m for linear model and 237 MV/m for model with dynamically changing Qo.

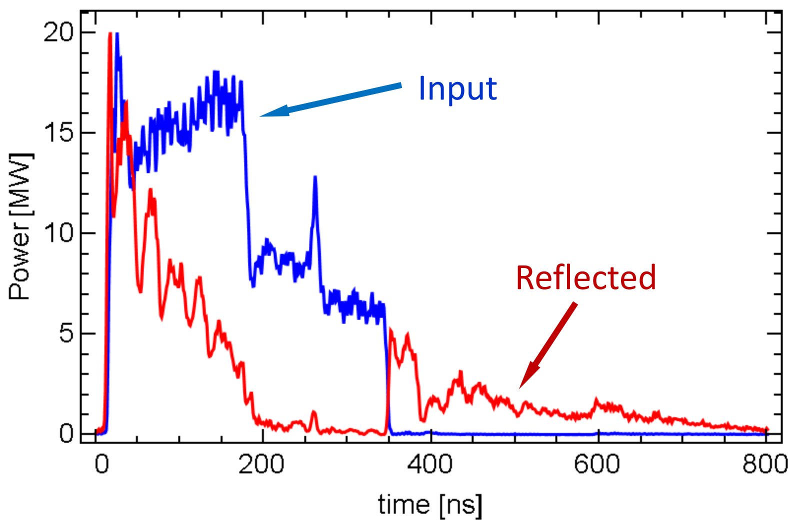

RF power vs. time

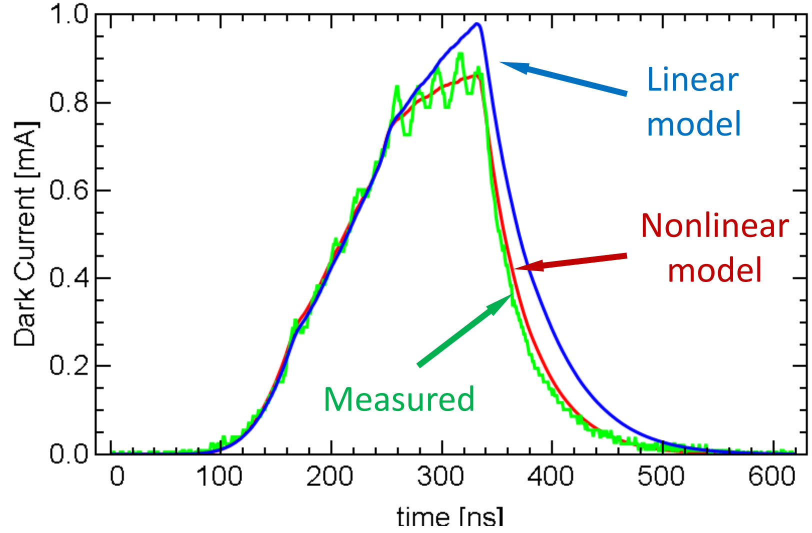

Dark current signal vs. time

Breakdown Rate Results using model with dynamic Qo to calculate the gradient, for *first breakdowns*

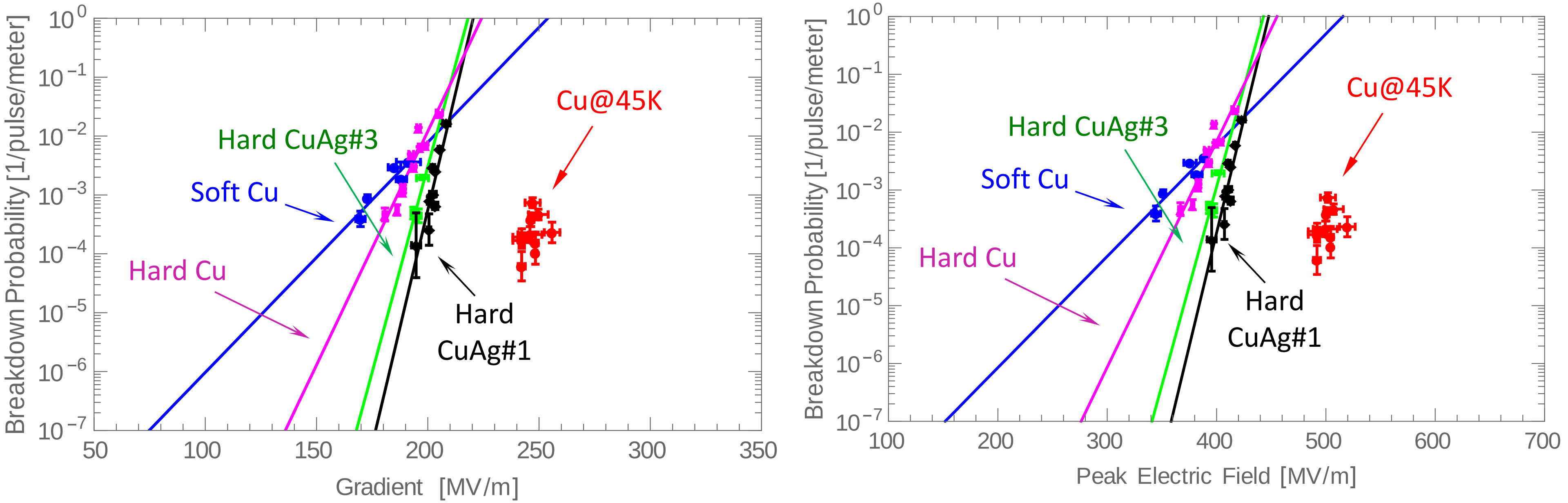

Breakdown rate *vs.* gradient and peak surface electric for first rf breakdowns, 1C-A2.75-T2.0 structures, shaped rf pulse with 150 ns flat part

A. Cahill *et al.*, "Ultra High Gradient Breakdown Rates in X-Band Cryogenic Normal Conducting Rf Accelerating Cavities," IPAC 17

Status of our Cryo Experiments

- Results of systematic study of Qo change in cryogenic accelerating cavity confirmed very high accelerating gradients. As for now, these are accelerating cavities with best high gradient performance.
- The major part of Qo change is consistent with beam loading due to dark currents. It is possible that the other mechanisms of rf losses (say resistivity increase with temperature) are also present, but the strong dependence of dark current from surface fields, likely dominates.
- Second X-band Structure will be tested in the coming months
- S-band cryostat and cavity is being designed and soon will go into manufacturing

TOPGUN: Collaboration on Next Generation RF Photoinjector

UCLA: J.B. Rosenzweig, A. Cahill, C. Emma, A. Fukusawa, R. Li, J. Maxson, P. Musumeci, A. Nause, R. Pakter, R. Roussel

SLAC: V.A. Dolgashev, C. Limborg, S. Tantawi

INFN-LNF: B. Spataro, R. Pompili

Next Generation Photo RF gun: Ultra-High Field Cryo "TopGun"

- S-band; drop-in for LCLS
- Operation at ~**27K** (liquid Ne)
- Peak cathode field **250 MV/m**
- Symmetrized Mode-Launcher coupler
- Overcoupled for short, **<1 usec pulses**
- Cavity shape is optimized for low heat load
- Short cathode cell for near 90° launch phase
- Launch field up from present in LCLS
  - 60 MV/m to 240 MV/m … x4!

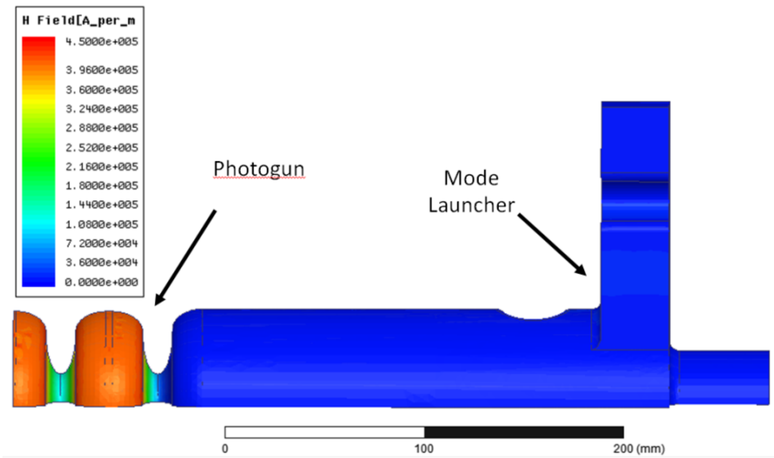

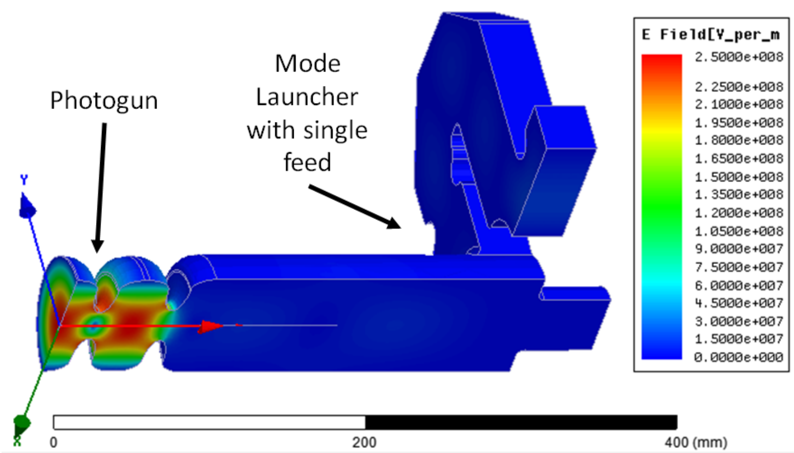

S-band RF Photogun Cavity Parameters

Internal quality factor Q_0 300 K	13, 483
Internal quality factor Q_0 27 K	62,425
Input power	50 MW
Normalized shunt impedance R/Q	136 Ω
Peak field at end of RF fill	250 MV/m
Fill time (β=9) β=2 at 300 K	0.9 μsec
Energy dissipated/pulse (τ=0.9 μs)	4.25 J (510 W at 120 Hz)

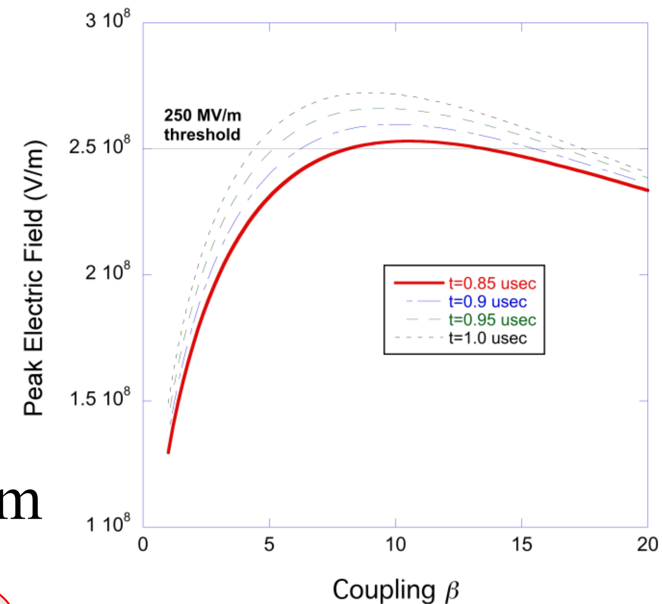

Power Handling and Cryo-cooler

- Asymptotic power in cavity: 18 MW
- Integrate power with time dependence

$$Pc = e^{-2t/tf} \qquad t_f = \frac{2Q_0}{\omega(1+\beta)} \approx 700ns$$

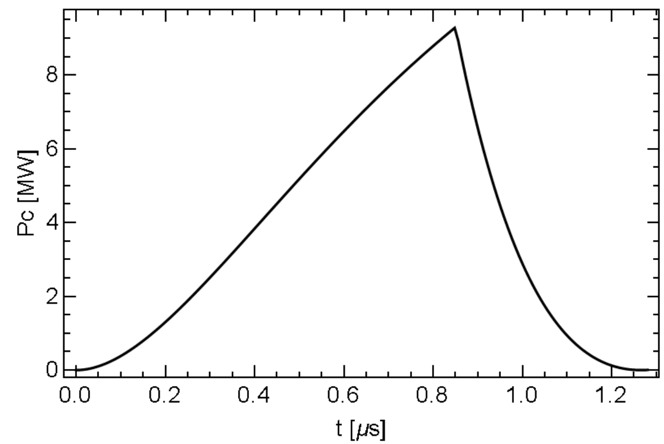

- Will remove field quickly by flipping phase on pulse.
- Pulse Heating: ~12 K
- Total power at 27 deg K, 120 Hz: 550 W
- Wall power of cryo-cooler: 35 kW
- Cost estimate for cryo-cooler: $650k (2 quotes)

Quadrupole-Free Mode Launcher

- Quadrupole Field Component reduced by 7 orders of magnitude for electron beams propagating left to right in bottom right image (when rf power is input into the rectangular waveguide on top).
- Physical Size is 400 mm x 175mm x 225mm

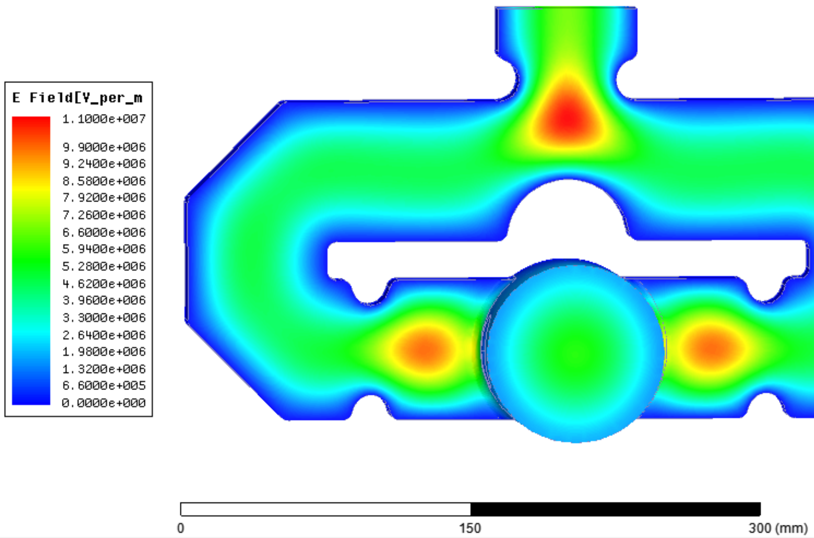

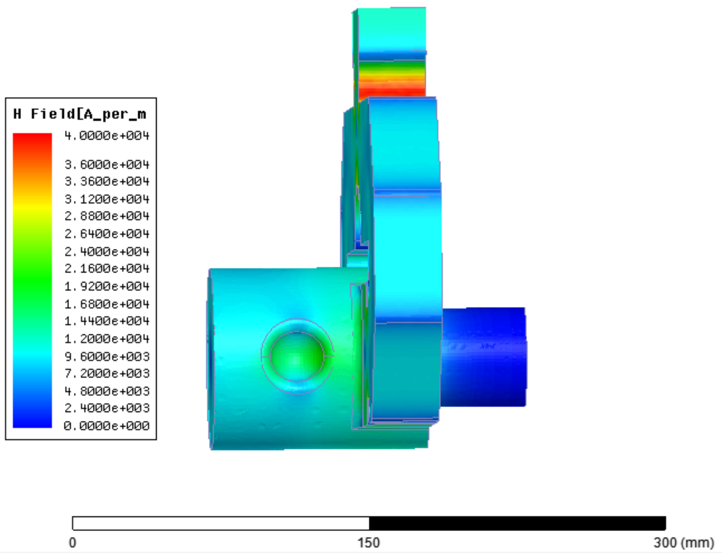

Fields normalized to 50MW input power

A. Cahill et al. **Measurements of Copper RF Surface Resistance at Cryogenic Temperatures for Applications to X-Band and S-Band Accelerators**. IPAC2015

What does this next gen device do? Beam Dynamics Studies

- GPT simulations with High charge blowout regime for FEL
- ~Standard solenoid focusing
- Emittance compensation, post accel. studied
- **Excellent results:** Extremely high potential impact on LCLS II with Start-to-end FEL simulations

UCLA-SLAC

Beam Acceleration, Transverse Envelope and Emittance

GPT simulations

Focusing with 2 kG solenoid, acceleration in linac starts at 1.7 m

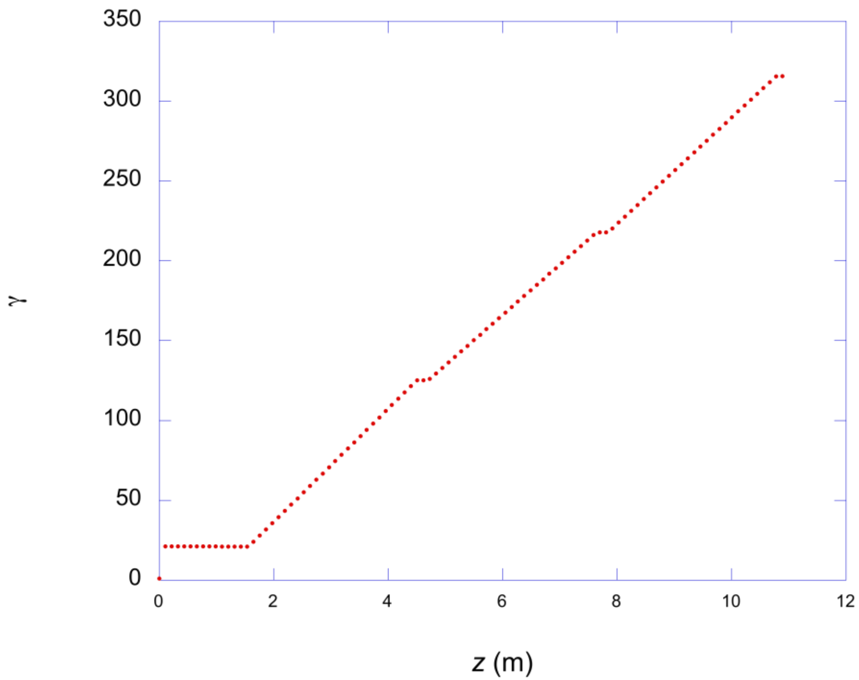

Acceleration to 161 MeV

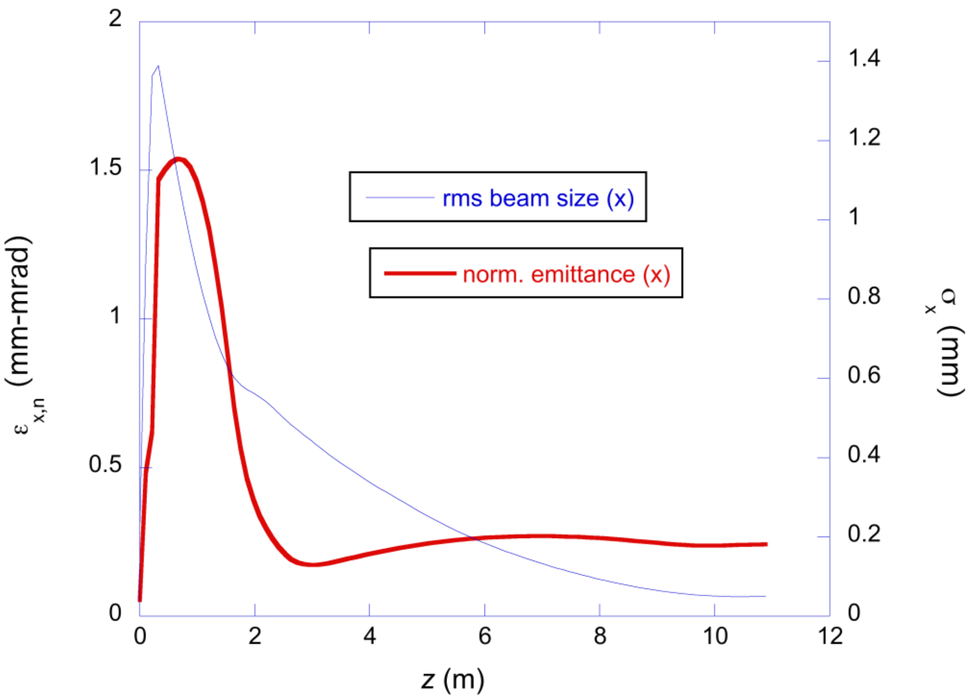

Emittance compensated finishes ~0.2 m-mrad

UCLA-SLAC

Longitudinal Expansion

- After gun, 10.5 MeV energy, ellipsoidal beam formed by longitudinal expansion

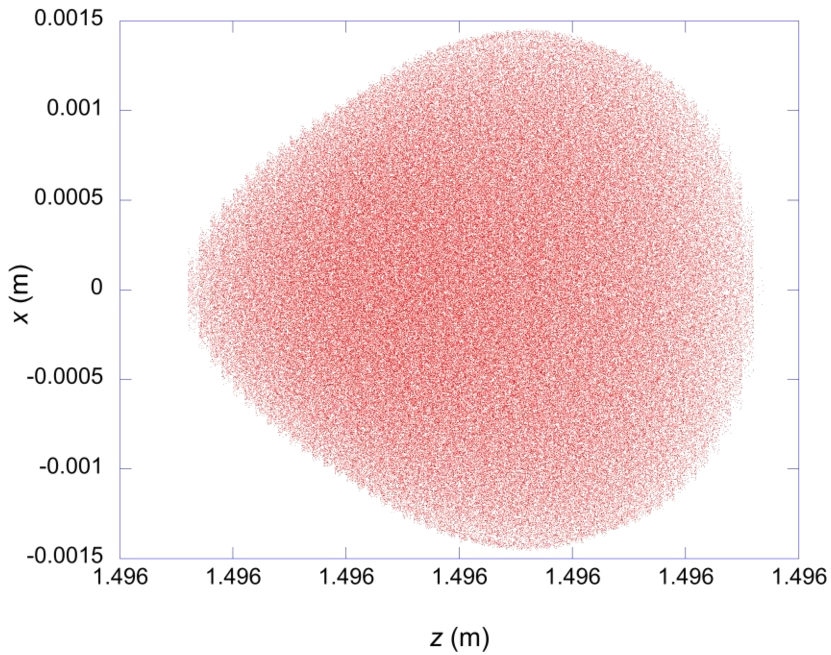

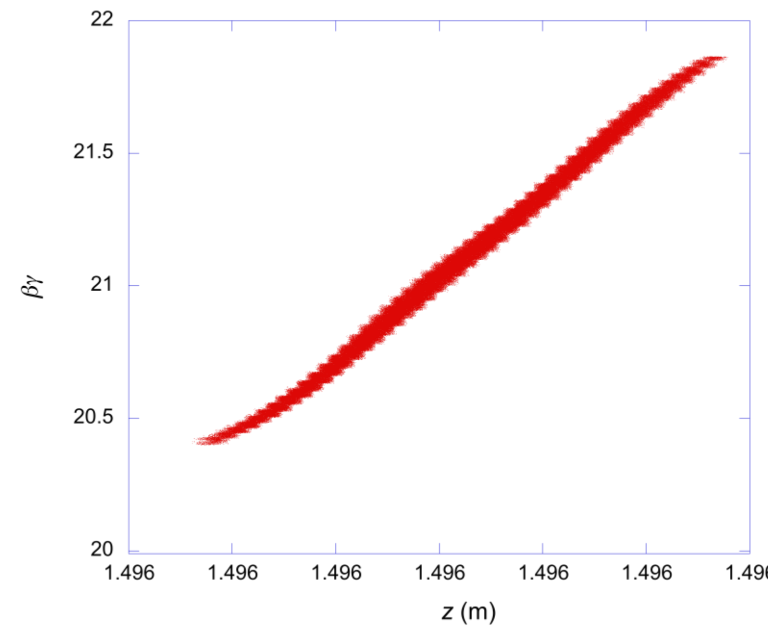

Projection (*x-z*) of ellipsoidal charge distribution due to blowout

Highly linear, compressible longitudinal phase space due to linear space charge fields

Parameters chosen to give 100A peak (original LCLS design comparison)

UCLA-SLAC

Start-to-End Simulations

- **GPT** to 160 MeV
  - Space charge

$$B_e = 5.2 \times 10^{17}\ \text{A/m-rad}^2$$

25x that of original LCLS design!

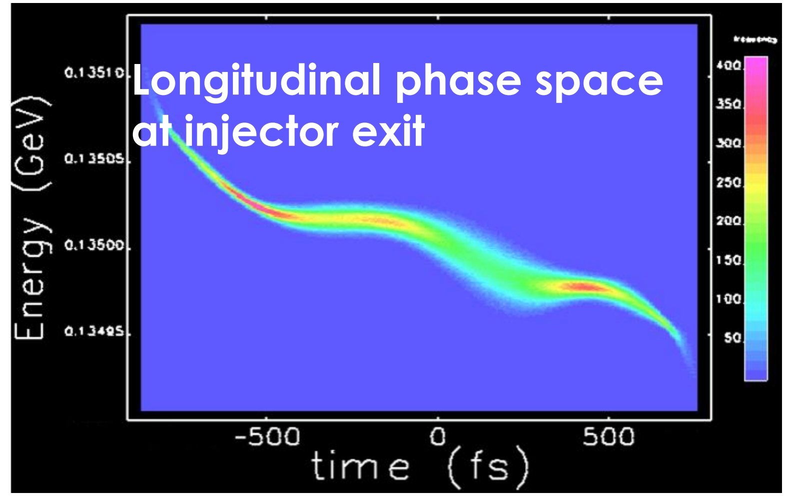

- **ELEGANT** for acceleration, compression and transport to undulator
- **GENESIS,** including tapering and self-seeding in LCLS

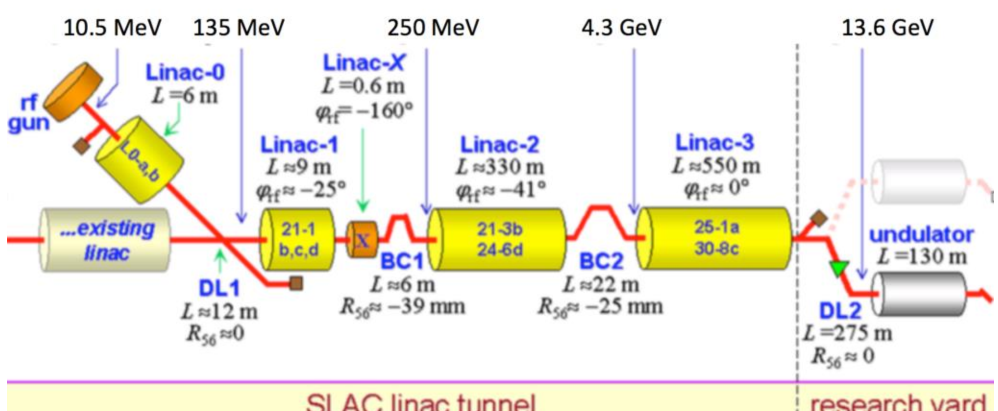

UCLA-SLAC

Acceleration and Compression: Elegant Simulations

- LCLS lattice, chicanes (benchmarked)
- 2.5 kA in beam core (usual peaks in wings)
- Slice emittance <.2 um

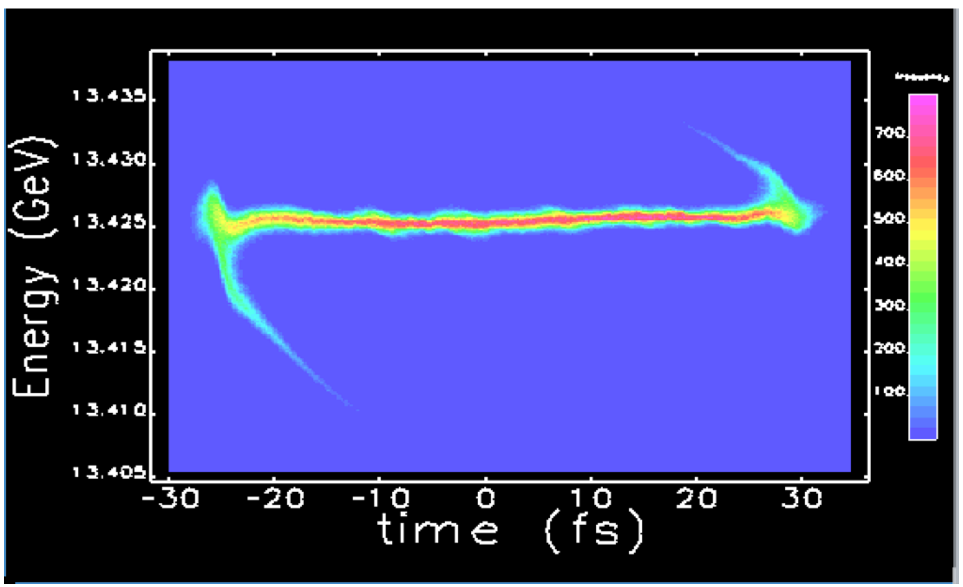

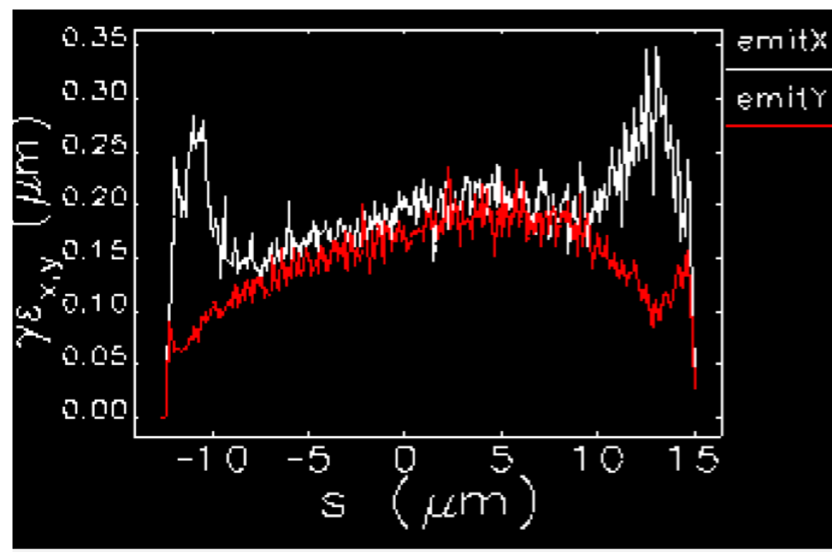

UCLA-SLAC

LCLS undulator GENESIS simulation:

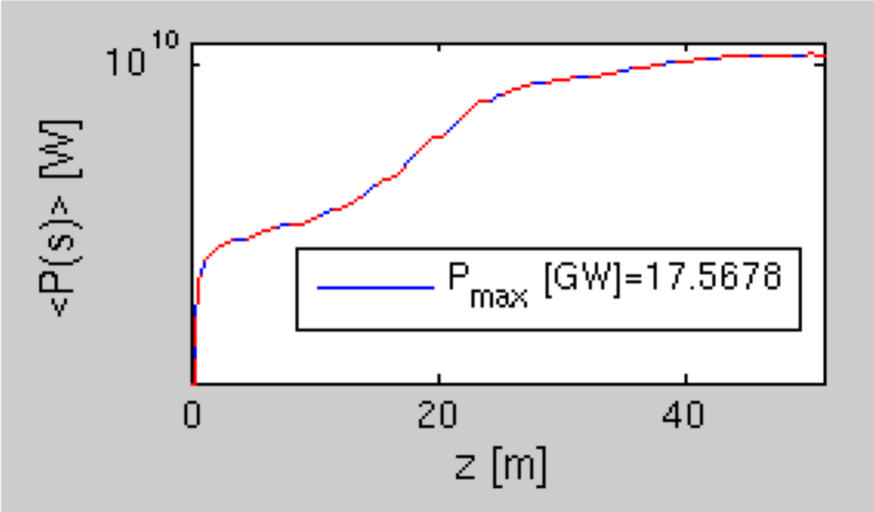

Saturation after 25 m

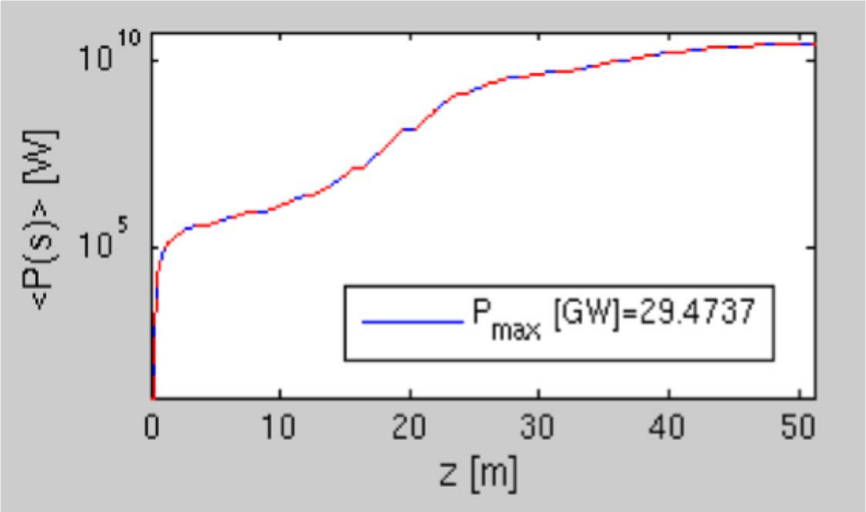

D*K*/*K*=0.1% tapering after 20 m

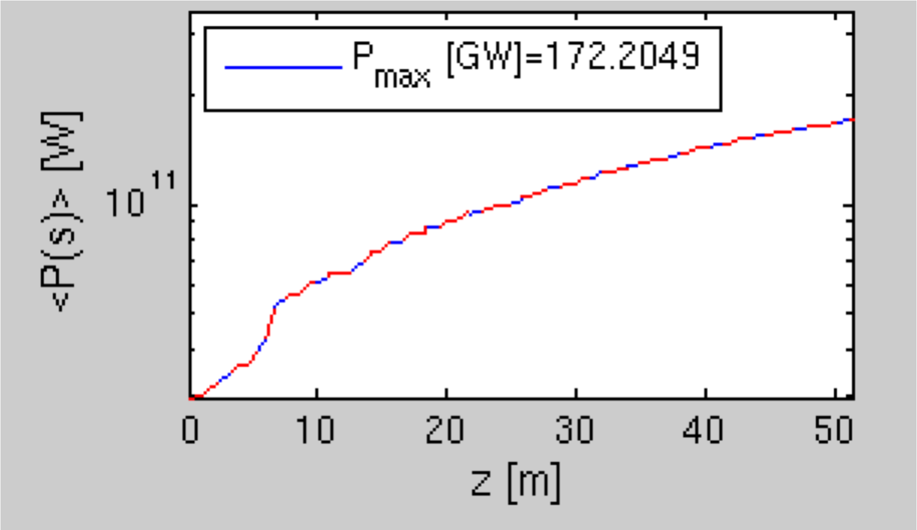

Maximum available at LCLS D*K*/*K*=0.8 after HXRsS

Pulse energy
8.5 mJ @ 125 pC

UCLA-SLAC

Advanced FEL case, 100 pC

- Long beam, **cigar regime**
- Full emittance ε_n=51 nm-rad
- Still space-charge dominant
  - Thermal ε_n=28 nm-rad
  - **Lower ε_n with solenoid changes**
- **Halo collimation helps**

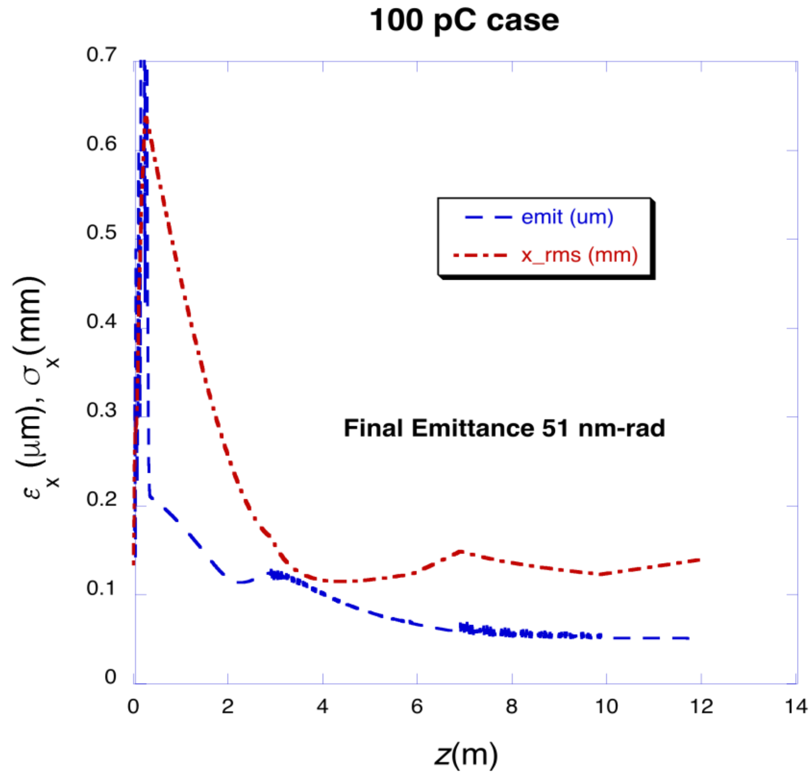

20% of ε_n is in 5%halo

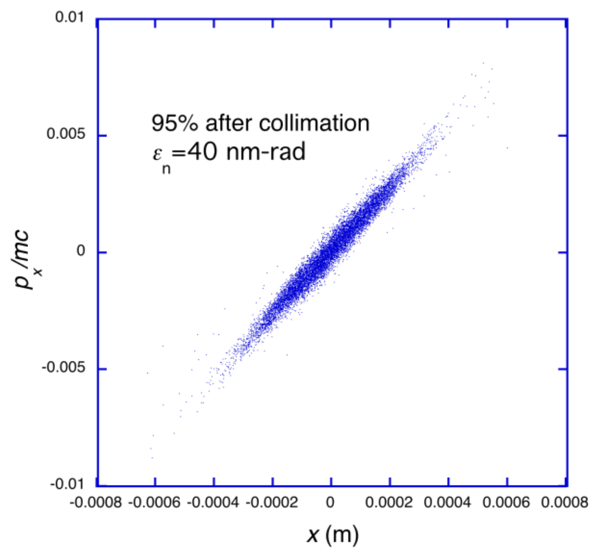

Final ε_n=40 nm w/collimation!
÷10 w.r.t. state-of-the-art

UCLA-SLAC

Can we transport and compress ultra-high brightness? CSR μ-Bunching is challenging

- **FEL-like instability is result of very bright electron beam**

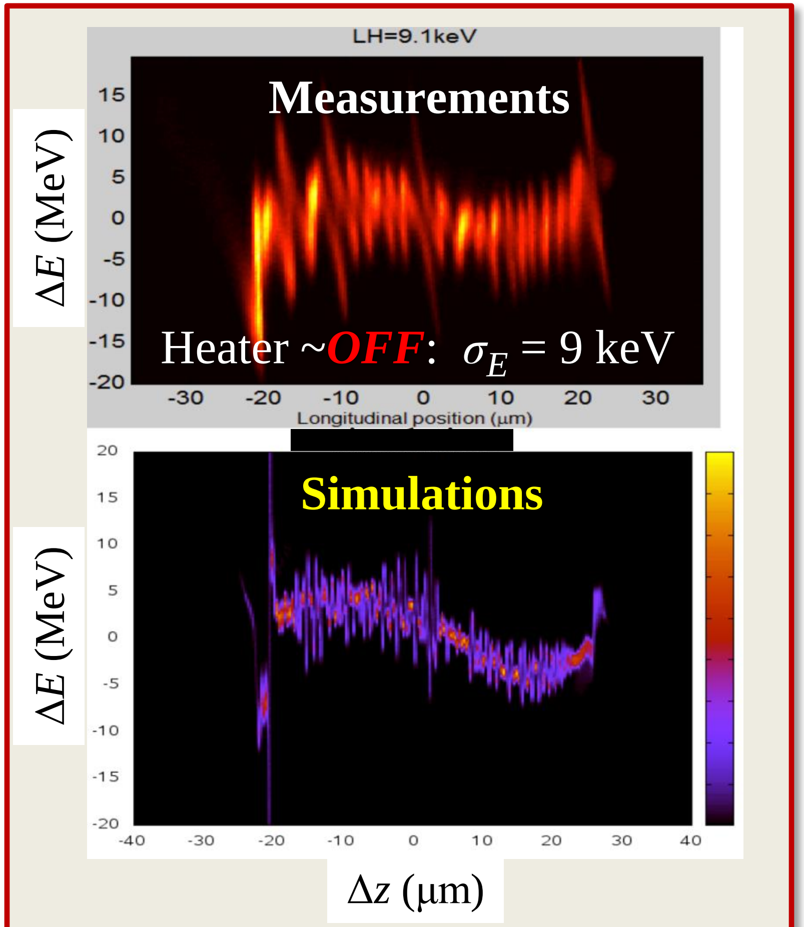

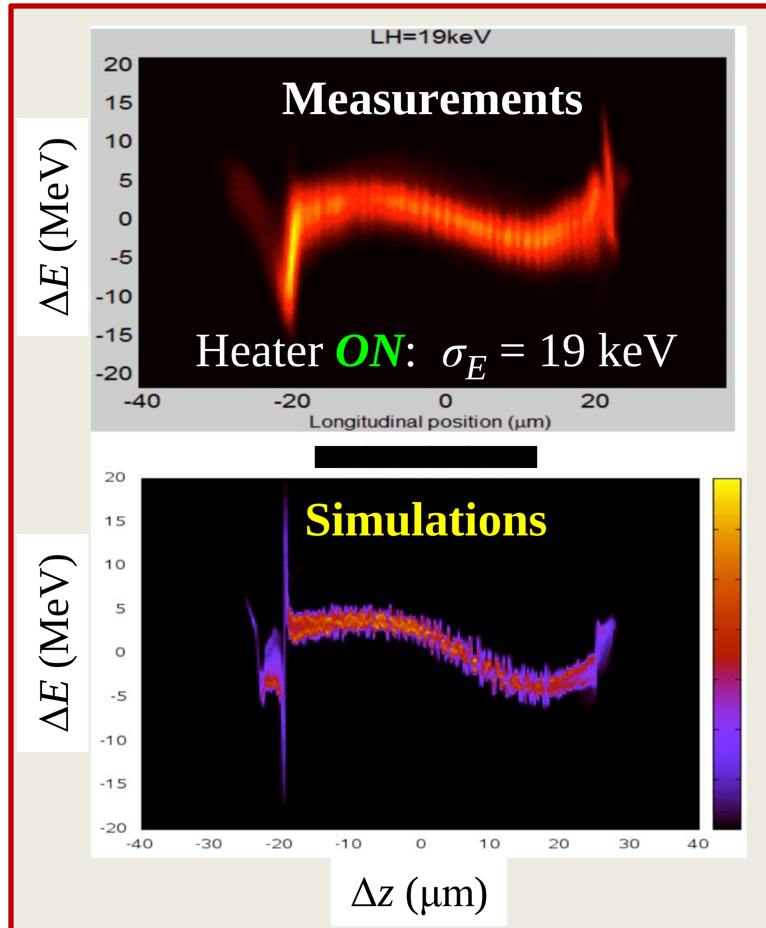

Simulations by J. Qiang, *LBNL* D. Ratner *et al*, Phys. Rev. ST Accel. Beams **18**, 030704 (2015).

Short λ_u ideal companion to **ESASE**

- Low average current, wakes

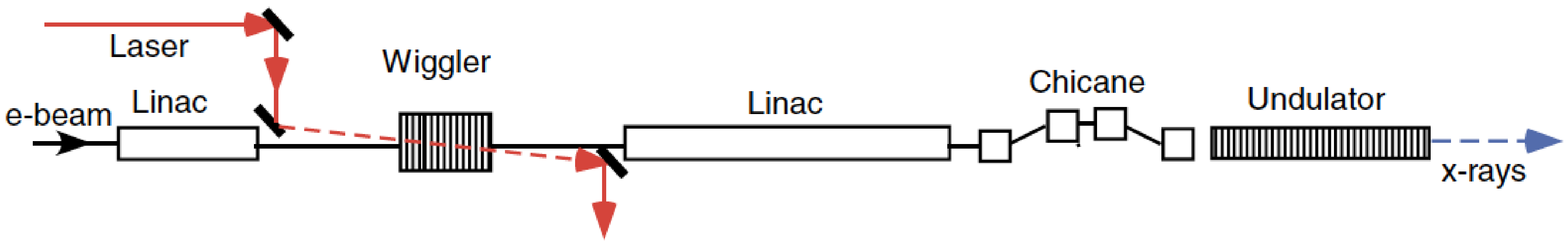

- **Avoids full beam compression**
  - **CSR ruins attained high brightness**
- Simulation of 100 pC case with superconducting undulator, K=1.8, period 9mm, gap 3mm.
- Existing LCLS infrastructure

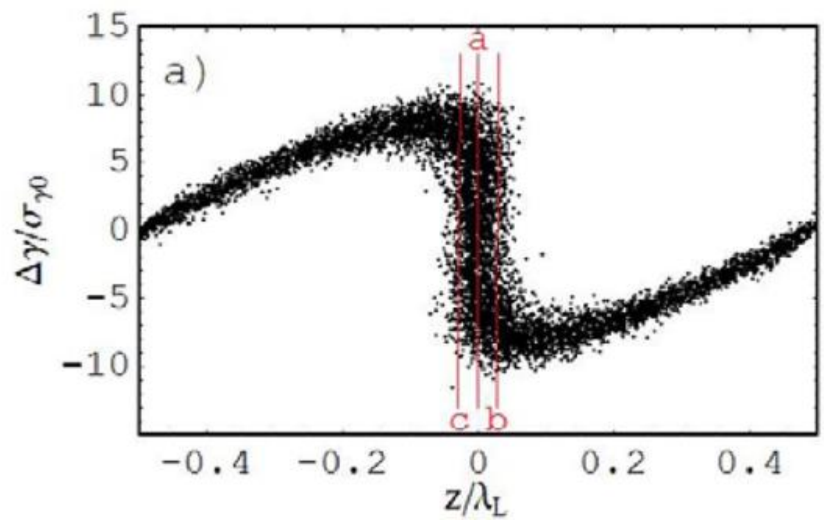

UCLA-SLAC

ESASE results encouraging

- Short period *superconducting undulator*
- Operation at *K*=1.8 gives **80 keV X-rays**
- Saturation in only 20 m, with 70 GW peak

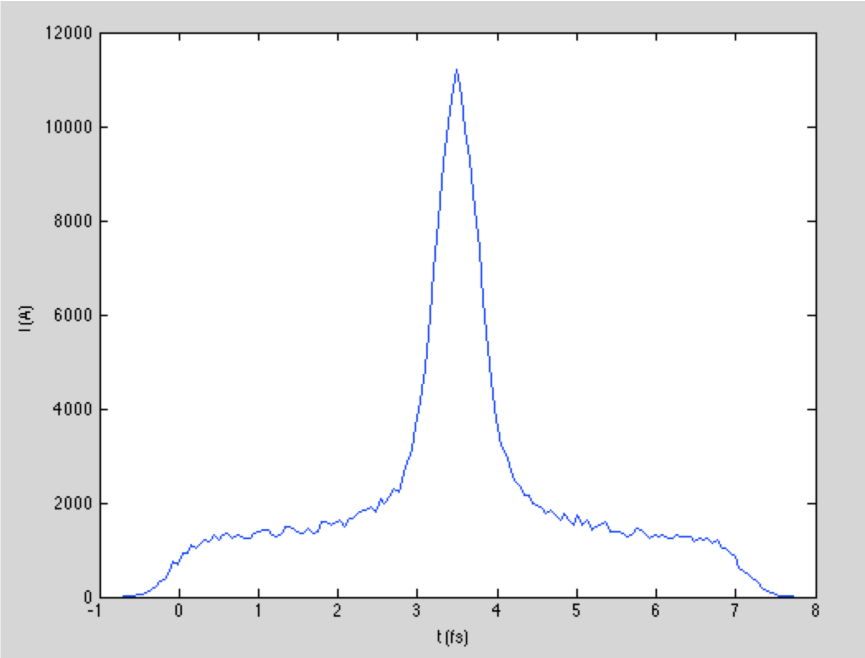

Current profile (10 kA)

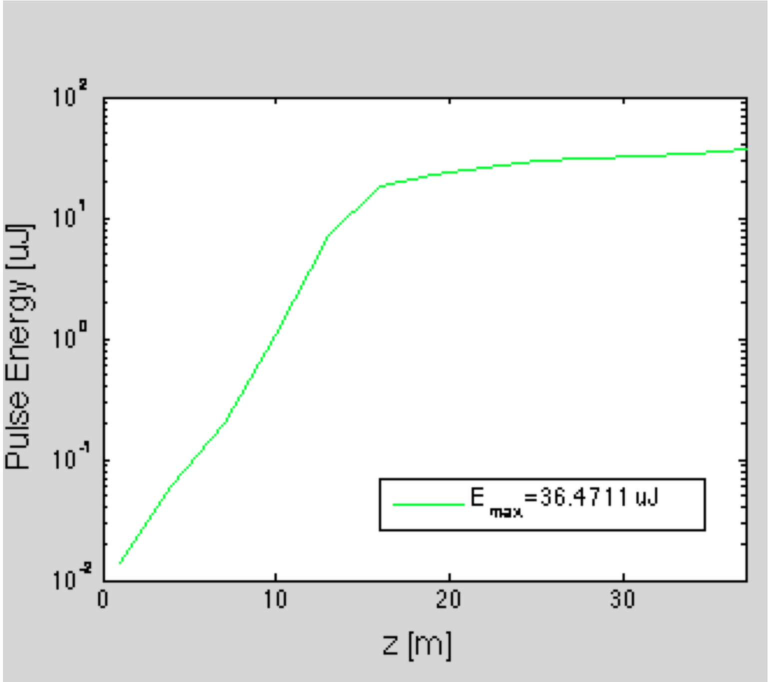

Energy evolution

UCLA-SLAC

Conclusion

Understanding of high gradient acceleration and advances in FEL physics open possibilities for building of practical compact light sources.